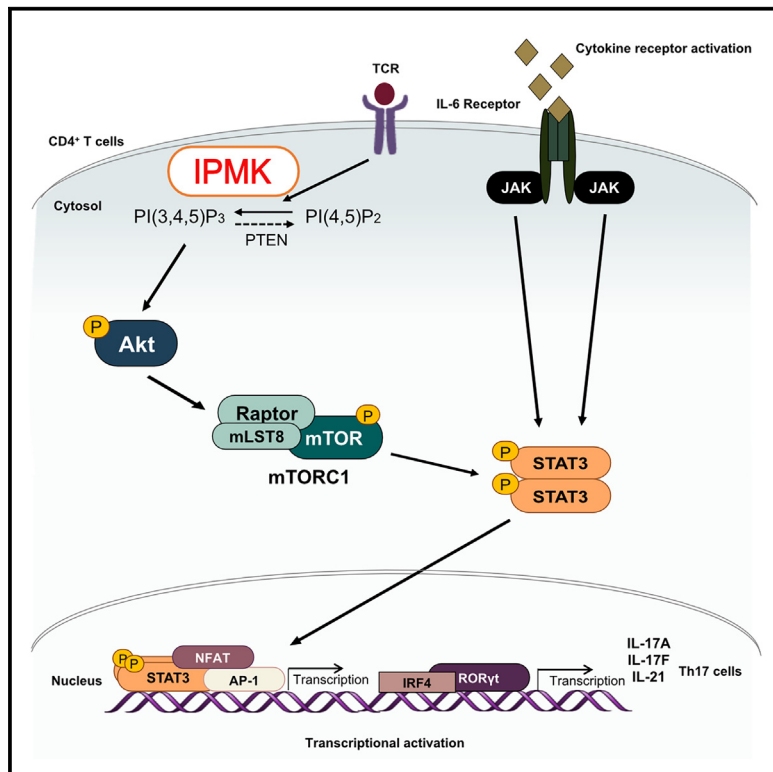


Inositol polyphosphate multikinase regulates Th1 and Th17 cell differentiation by controlling Akt-mTOR signaling

Graphical abstract



Authors

Chae Min Yuk, Sehoon Hong,
Dongeon Kim, ..., Rho Hyun Seong,
Seyun Kim, Seung-Hyo Lee

Correspondence

rhseong@snu.ac.kr (R.H.S.),
seyunkim@kaist.ac.kr (S.K.),
sl131345@kaist.ac.kr (S.-H.L.)

In brief

Yuk et al. demonstrated that conditional deletion of IPMK in CD4⁺ T cells leads to reduced Th1- and Th17-mediated immunity in mice, thereby controlling *Leishmania major* infection and experimental autoimmune encephalomyelitis. Mechanistically, the catalytic function of IPMK as a PI3-kinase regulates CD4⁺ T cell differentiation by activating Akt-mTOR-STAT signaling.

Highlights

- IPMK plays a key role in Th1- and Th17-dependent immune reactions in mice
- Deletion of IPMK in CD4⁺ T cells reduces Akt and its downstream mTOR and STAT activation
- IPMK is a physiological PI3-kinase responsible for the production of PIP₃ in CD4⁺ T cells
- Targeting IPMK may assist in the treatment of infections as well as autoimmune disorders



Article

Inositol polyphosphate multikinase regulates Th1 and Th17 cell differentiation by controlling Akt-mTOR signaling

Chae Min Yuk,^{1,13,15} Sehoon Hong,^{2,15} Dongeon Kim,^{1,3,6,7,15} Mingyo Kim,⁸ Hyun-Woo Jeong,^{9,10} Seung Ju Park,² Hyungyu Min,¹¹ Wooseob Kim,^{11,14} Jongbu Lim,² Hyo Dam Kim,² Sang-Gyu Kim,² Rho Hyun Seong,^{11,*} Seyun Kim,^{2,4,5,*} and Seung-Hyo Lee^{1,3,12,16,*}

¹Graduate School of Medical Science and Engineering, Korea Advanced Institute of Science and Technology (KAIST), Yuseong-Gu, Daejeon 34141, Republic of Korea

²Department of Biological Sciences, Korea Advanced Institute of Science and Technology (KAIST), Yuseong-Gu, Daejeon 34141, Republic of Korea

³Biomedical Research Center, Korea Advanced Institute of Science and Technology (KAIST), Yuseong-Gu, Daejeon 34141, Republic of Korea

⁴KAIST Institute for the BioCentury, Korea Advanced Institute of Science and Technology (KAIST), Yuseong-Gu, Daejeon 34141, Republic of Korea

⁵KAIST Stem Cell Center, Korea Advanced Institute of Science and Technology (KAIST), Yuseong-Gu, Daejeon 34141, Republic of Korea

⁶Department of Medicine, Stanford University School of Medicine, Stanford, CA 94305, USA

⁷VA Palo Alto Health Care System, Stanford University School of Medicine, Stanford, CA 94305, USA

⁸Division of Rheumatology, Department of Internal Medicine, Gyeongsang National University Hospital, Jinju 52727, Republic of Korea

⁹Department of Tissue Morphogenesis, Max Planck Institute for Molecular Biomedicine, 48149 Münster, Germany

¹⁰Faculty of Medicine, University of Münster, 48149 Münster, Germany

¹¹School of Biological Sciences and Institute of Molecular Biology and Genetics, Seoul National University, Seoul 08826, Republic of Korea

¹²Department of Medicine, College of Medicine, Korea University, Seoul 02841, Republic of Korea

¹³Present address: Center for Vascular Research, Institute for Basic Science, Daejeon 34141, Republic of Korea

¹⁴Present address: Department of Microbiology, Korea University College of Medicine, Seoul 02841, Republic of Korea

¹⁵These authors contributed equally

¹⁶Lead contact

*Correspondence: rhseong@snu.ac.kr (R.H.S.), seyunkim@kaist.ac.kr (S.K.), sl131345@kaist.ac.kr (S.-H.L.)

<https://doi.org/10.1016/j.celrep.2025.115281>

SUMMARY

Activated proinflammatory T helper (Th) cells, including Th1 and Th17 cells, drive immune responses against pathogens and contribute to autoimmune diseases. We show that the expression of inositol polyphosphate multikinase (IPMK), an enzyme essential for inositol phosphate metabolism, is highly induced in Th1 and Th17 subsets. Deletion of IPMK in CD4⁺ T cells leads to diminished Th1- and Th17-mediated responses, reducing resistance to *Leishmania major* and attenuating experimental autoimmune encephalomyelitis. IPMK-deficient CD4⁺ T cells show impaired activation and Th17 differentiation, linked to the decreased activation of Akt, mTOR, and STAT3. Mechanistically, IPMK functions as a phosphatidylinositol 3-kinase to regulate phosphatidylinositol (3,4,5)-trisphosphate (PtdIns(3,4,5)P₃) production, promoting T cell activation and effector functions. In IPMK-deficient CD4⁺ T cells, T cell receptor-stimulated PtdIns(3,4,5)P₃ generation is abolished by wortmannin, suggesting IPMK acts in a wortmannin-sensitive manner. These findings establish IPMK as a critical regulator of Th1 and Th17 differentiation, underscoring its role in maintaining immune homeostasis.

INTRODUCTION

CD4⁺ T helper (Th) cells not only play critical roles in mediating adaptive immune responses to various pathogens but are also involved in allergic responses, autoimmunity, and tumor immunity. Naive CD4⁺ T cells become effector and/or memory cells with specialized phenotypes, including Th1, Th2, Th17, and regulatory T (Treg) cells, as defined by signature cytokines and master transcription factors. Interleukin (IL)-12 and interferon (IFN)- γ are major inducers of Th1 cells, while the master transcriptional regulator for Th1 cells is T-bet. While the induction of T-bet is

dependent on signaling transducer and activator of transcription 1 (STAT1), IL-12 signaling activates STAT4. IL-4 is a critical cytokine for Th2 cell differentiation, and IL-4-induced STAT6 upregulates the expression of the Th2 cell master regulator, GATA3. Th17 cells develop in the presence of IL-6, transforming growth factor β (TGF- β), IL-21, and IL-23, which induce the upregulation of the master regulator retinoic acid receptor-related orphan gamma T (ROR γ T) through STAT3. In addition, Treg cells express the master transcription factor, Foxp3, and develop in peripheral lymphoid organs after antigen priming (induced Treg; iTreg) or in the thymus (natural Treg; nTreg).¹



Th1 cells are required for the immune responses against intracellular pathogens, such as viruses and intracellular bacteria, and exert their effects through the secretion of IFN- γ , which activates macrophages for enhanced phagocytic function. However, uncontrolled Th1-mediated responses cause autoimmunity by inducing chronic inflammatory responses as well as Th17 cells. Th17 cells, characterized by the production of signature cytokines IL-17A, IL-17F, and IL-22, are thought to be critically involved in infection, inflammation, autoimmunity, and cancer.^{2–4} Dysregulated Th17 cells play roles in the development of various autoimmune diseases, including psoriasis, inflammatory bowel disease, rheumatoid arthritis, and multiple sclerosis.⁵ Further, STAT3, activated by IL-6, functions as a promoter of *Rorc*, *Il17a*, *Il17f*, and multiple other genes associated with Th17 cell polarization and survival.⁶ Consequently, IL-17 causes granulopoiesis by inducing granulocyte colony-stimulating factor (GM-CSF) secretion in the stroma of bone marrow and promotes the expression of tumor necrosis factor alpha (TNF- α), IL-1 β , IL-6, chemokines, and the GM-CSF receptor.^{7,8} Therefore, IL-17 is highly pleiotropic and induces a range of inflammatory effects that link innate and adaptive immunity. As a result, Th17 cells cause tissue damage by recruiting neutrophils and macrophages into peripheral tissues.

Upon antigen presentation, T cell receptors (TCRs) and costimulatory molecules trigger signaling pathways, including the activation of phosphatidylinositol 3-kinase (PI3K), which leads to the phosphorylation on the third position of phosphatidylinositol(4,5)-bisphosphate (PIP₂) to produce phosphatidylinositol(3,4,5)-trisphosphate (PIP₃), a potent second messenger known to promote Akt activities.^{9,10} Subsequently, mechanistic target of rapamycin (mTOR) complex 1 (mTORC1) becomes stimulated, thereby positively governing Th cell differentiation via downstream signaling factors such as S6K.¹¹ PI3K-Akt-mTORC1 signaling also induces expression of hypoxia-inducible factor-1 α (HIF-1 α) downstream of mTORC1,^{12,13} and in turn, HIF-1 α positively regulates Th17 cell differentiation by enhancing Th17-related genes such as ROR γ t and the glycolytic activity needed to expand T cells.^{12,14} In addition, mTORC1 regulates the phosphorylation of STAT proteins during Th1 and Th17 cell differentiation.¹⁵ Moreover, deletion of *Rheb*, resulting in the dysfunction of mTORC1, selectively reduces the tyrosine phosphorylation of STAT3 and STAT4, which are downstream signaling molecules of IL-6 and IL-12, respectively.¹⁵

Inositol polyphosphate multikinase (IPMK) is a pleiotropic enzyme essential for the production of inositol polyphosphates (InsPs), such as InsP₄ and InsP₅.¹⁶ With broad substrate specificity, IPMK is also known to display PI3K activity, which forms the second messenger PIP₃ by phosphorylating PIP₂.^{17,18} IPMK deletion in mouse embryonic fibroblasts (MEFs) was shown to decrease cellular PIP₃ levels as well as significantly reduce PIP₃-dependent Akt phosphorylation in response to growth factors, suggesting that IPMK is a physiological PI3K.¹⁸ Recently, it is revealed that single-nucleotide polymorphisms (SNPs) in IPMK are associated with immune-mediated diseases such as Crohn's disease.¹⁹ Moreover, IPMK coordinates the activity of various biological events in different cell types. In myeloid cells, IPMK was recently shown to control Toll-like receptor signaling, and in B cells, this kinase is necessary for the full activation of Btk

signaling.^{20,21} Accordingly, we asked whether IPMK also plays a critical role in T cell-mediated immune responses. Here, we demonstrate that IPMK plays a key role in Th1- and Th17-dependent immune reactions by controlling Akt-mTOR signaling. Conditional deletion of IPMK in murine CD4 $^+$ T cells blunts immune homeostasis dependent on Th1 and Th17, but not Th2, cells, rendering mice more susceptible to *Leishmania major* infection and less susceptible to experimental autoimmune encephalomyelitis (EAE). Further, we show that IPMK deletion impairs Th1 and Th17 cell differentiation, which is associated with reduced production of PIP₃, leading to a marked reduction of Akt and its downstream signaling events during T cell activation and differentiation. We also demonstrate that treatment with wortmannin, a potent classical PI3K inhibitor, nearly impairs PIP₃ synthesis in IPMK-deficient CD4 $^+$ T cells upon TCR stimulation. Thus, our results identify IPMK as a physiological PI3K of Th1 and Th17 cells.

RESULTS

Increased expression of IPMK by Th1 and Th17 cells

To address whether IPMK is expressed in effector CD4 $^+$ T cells, we sorted naive CD4 $^+$ CD62L $^+$ CD25 $^-$ CD44 $^+$ T cells from wild-type (WT) mice by fluorescence-activated cell sorting (FACS) and differentiated them into Th1, Th2, and Th17 cells. While Th2 cells modestly express IPMK, IPMK expression is highly up-regulated in Th1 and Th17 cells (Figure S1). Because IPMK is highly expressed in Th1 and Th17 effector cells, we generated CD4 $^+$ T cell-specific *lpmk*-deficient mice by crossing *lpmk*-floxed mice (*lpmk*^{f/f}) with *Cd4*-Cre mice (Figure S2A) to investigate the function of IPMK in CD4 $^+$ T cell-mediated immunity. We confirmed that the expression of IPMK is absent in CD4 $^+$ T cells in CD4-specific *lpmk*-deficient (*lpmk*^{ΔCD4}) mice (Figure S2B). To investigate the effects of IPMK on T cell development, we analyzed the phenotypes of T cells in the thymus, peripheral lymph node (pLN), and spleen. Compared with WT controls (*lpmk*^{f/f}), *lpmk*^{ΔCD4} mice showed normal proportions of double-positive (CD4 $^+$ CD8 $^+$) T cells in the thymus and CD4 $^+$ or CD8 $^+$ single-positive T cells in the thymus, pLN, and spleen (Figures S3A and S3B). Further, the proportions of naive (CD62L hi CD44 lo) and effector/memory (CD62L lo CD44 hi) CD4 $^+$ and CD8 $^+$ T cells in the pLN and spleen were similar between *lpmk*^{f/f} and *lpmk*^{ΔCD4} mice (Figures S3C and S3D). Thus, the development of T cells is normal in CD4 $^+$ T cell-specific *lpmk* deletion.

Reduced Th1 immunity in the absence of IPMK in CD4 $^+$ T cells

Because IPMK is highly expressed in Th1 cells (Figure S1), we next investigated the importance of IPMK in Th1-mediated immune responses. For this, we infected *lpmk*^{f/f} and *lpmk*^{ΔCD4} mice with *L. major*, an intramacrophage parasite controlled by type 1 immunity in the host.²² *L. major* promastigotes were inoculated into the hind footpads, and the progression of lesion swelling was measured for 7 weeks after infection (Figure 1A). WT BALB/c mice were used for infection control. Compared with *lpmk*^{f/f} mice, *lpmk*^{ΔCD4} mice showed increased footpad thickness, which indicates decreased Th1-mediated immune responses. On the other hand, BALB/c mice were more

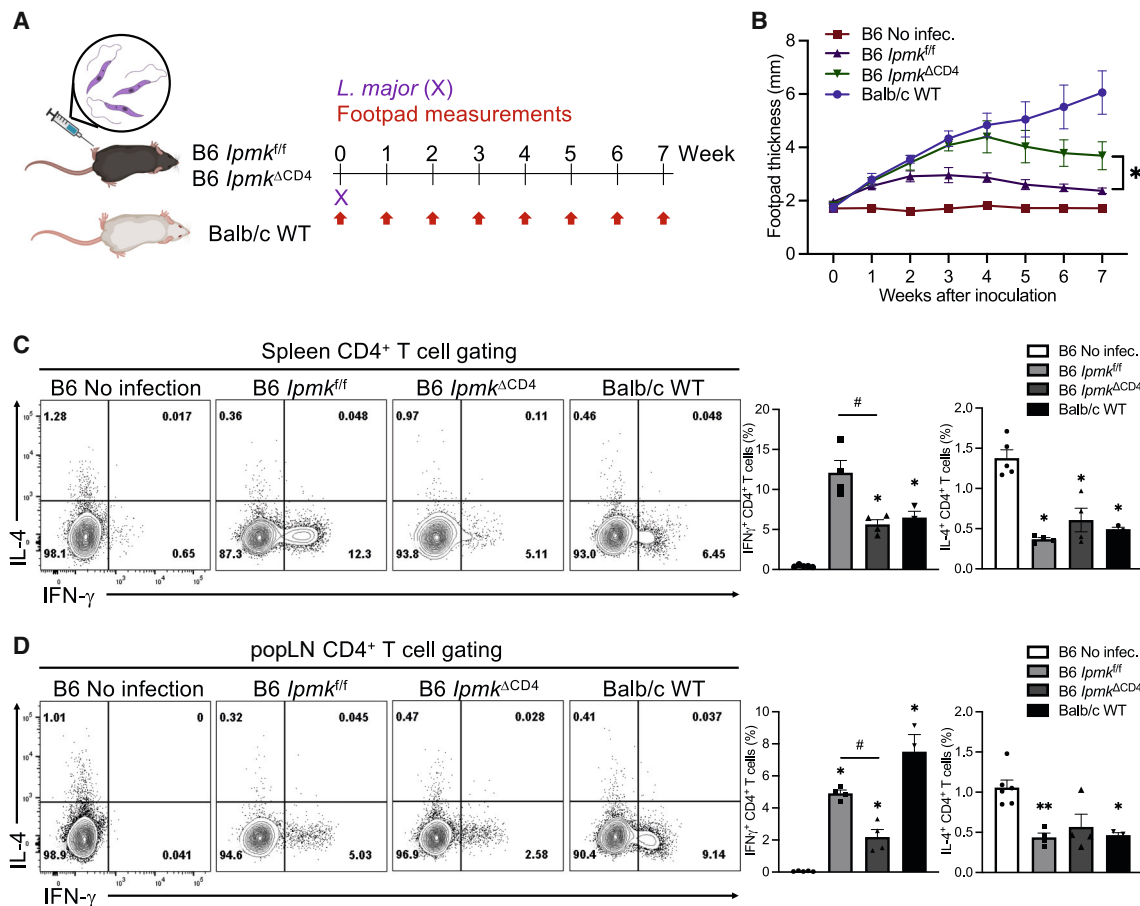


Figure 1. CD4⁺ T cell-specific IPMK deficiency shows reduced Th1-mediated immune responses against infection with *L. major*

(A–D) Mice were infected with 1×10^6 *L. major* promastigotes in the left hind footpad.

(A) Schematic diagram of the experimental protocol.

(B) The footpad swelling was monitored weekly, and footpad lesions were measured in mice with no infection (■), *lpmk*^{f/f} (▲) and *lpmk*^{ΔCD4} (▼) in C57BL/6 mice with infection, and Balb/c (●) mice with infection.

(C) Flow cytometric analysis were performed 7 weeks after infection from spleens. Representative flow cytometric plots and quantification of IFN- γ ⁺ and IL-4⁺ in CD4⁺ T cells are shown.

(D) Flow cytometric analyses were performed 7 weeks after infection from popliteal lymph nodes (popLNs). Representative flow cytometric plots and quantification of IFN- γ ⁺ and IL-4⁺ in CD4⁺ T cells are shown.

Data are presented as the mean \pm SEM; * p < 0.05 and ** p < 0.01 compared with the no infection group by the Mann-Whitney test. # p < 0.05 compared with the *lpmk*^{f/f} group by the Mann-Whitney test. See also Figure S1.

susceptible, as this strain of mice predominantly mounts Th2-mediated immune responses (Figure 1B). Because IFN- γ -production by CD4⁺ T cells is critical for the control of *L. major*,²³ we performed intracellular cytokine staining on cells from spleens and popliteal lymph nodes (popLNs) 7 weeks after infection. The IFN- γ ⁺ Th1 population was reduced in the spleen and popLN of *L. major*-infected *lpmk*^{ΔCD4} mice (Figures 1C and 1D). Thus, these data indicate that IPMK deficiency in CD4⁺ T cells dampens the protective Th1 immunity against *L. major* infection, decreasing parasite clearance. This emphasizes the importance of IPMK in Th1 immunity.

Decreased Th17 cell function due to IPMK deficiency

Next, we investigated the role of IPMK in Th17 cell differentiation and function. For this, we utilized an EAE model in which

Th17 cells are known to be critically involved in disease pathogenesis (Figure 2A). Following immunization with the neuro-antigen MOG_{35–55} peptide, *lpmk*^{ΔCD4} mice showed attenuated disease severity compared with *lpmk*^{f/f} mice (Figure 2B). Histological analysis showed decreased accumulation of infiltrating immune cells and resultant demyelination in the spinal cord of *lpmk*^{ΔCD4} mice compared with that of *lpmk*^{f/f} mice (Figure 2C). In addition, infiltration of inflammatory mononuclear cells, including CD4⁺ T cells, CD8⁺ T cells, neutrophils, macrophages, and B cells, into the central nervous system (CNS) was decreased in *lpmk*^{ΔCD4} mice compared with that of *lpmk*^{f/f} mice (Figures 2D and 2E). Indeed, the immunological analysis revealed that there were fewer CNS-infiltrating IL-17A⁺ and IFN- γ ⁺ CD4⁺ T cells in *lpmk*^{ΔCD4} mice than *lpmk*^{f/f} mice (Figure 2F). These findings indicate that IPMK is required

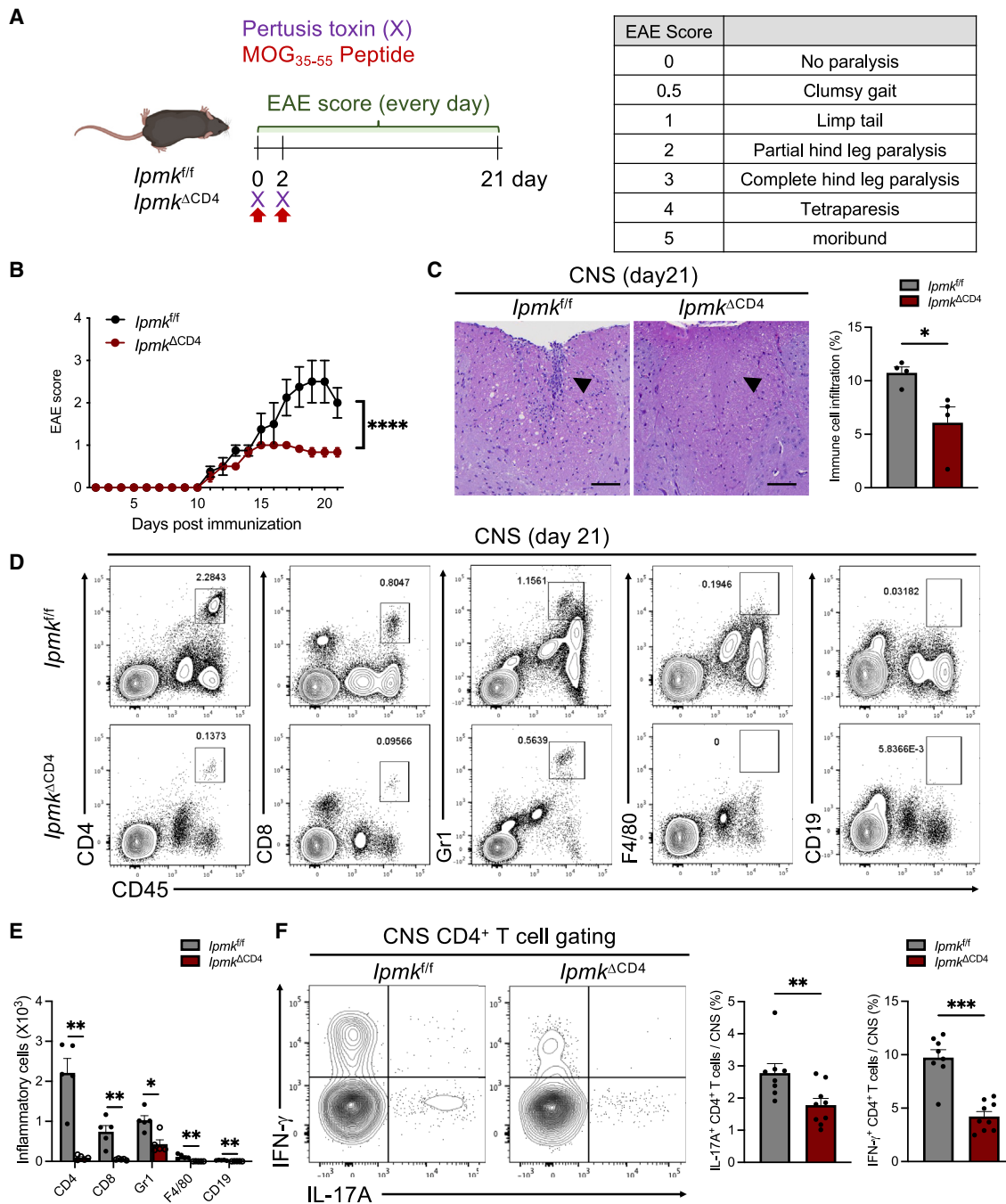


Figure 2. *lpmk^{ΔCD4}* mice protected from EAE

(A) Schematic diagram of the experimental protocol.

(B) Mean clinical score for EAE in *lpmk^{ff}* or *lpmk^{ΔCD4}* mice induced by immunization with MOG₃₅₋₅₅.

(C) Hematoxylin and eosin (H&E) staining from *lpmk^{ff}* or *lpmk^{ΔCD4}* mice harvested at the peak of disease. Scale bar, 100 μ m.

(D) Immune cell infiltration in the brains of MOG₃₅₋₅₅-immunized *lpmk^{ff}* or *lpmk^{ΔCD4}* mice harvested at the peak of disease analyzed by flow cytometry with antibodies to the indicated proteins.

(E) Absolute numbers of mononuclear CNS-infiltrating cells in harvested brains and spinal cords determined at the peak of disease by staining with antibodies to the indicated cell markers and subsequent flow cytometry.

(F) Flow cytometry of IL-17A or IFN- γ production of spinal cord from *lpmk^{ff}* or *lpmk^{ΔCD4}* mice ($n \geq 8$ per each group).

Each image shows representative and compiled data. Data are presented as the mean \pm SEM; ** $p < 0.01$, *** $p < 0.001$, and **** $p < 0.0001$ compared with the *lpmk^{ff}* group by the Mann-Whitney test. See also Figure S4.

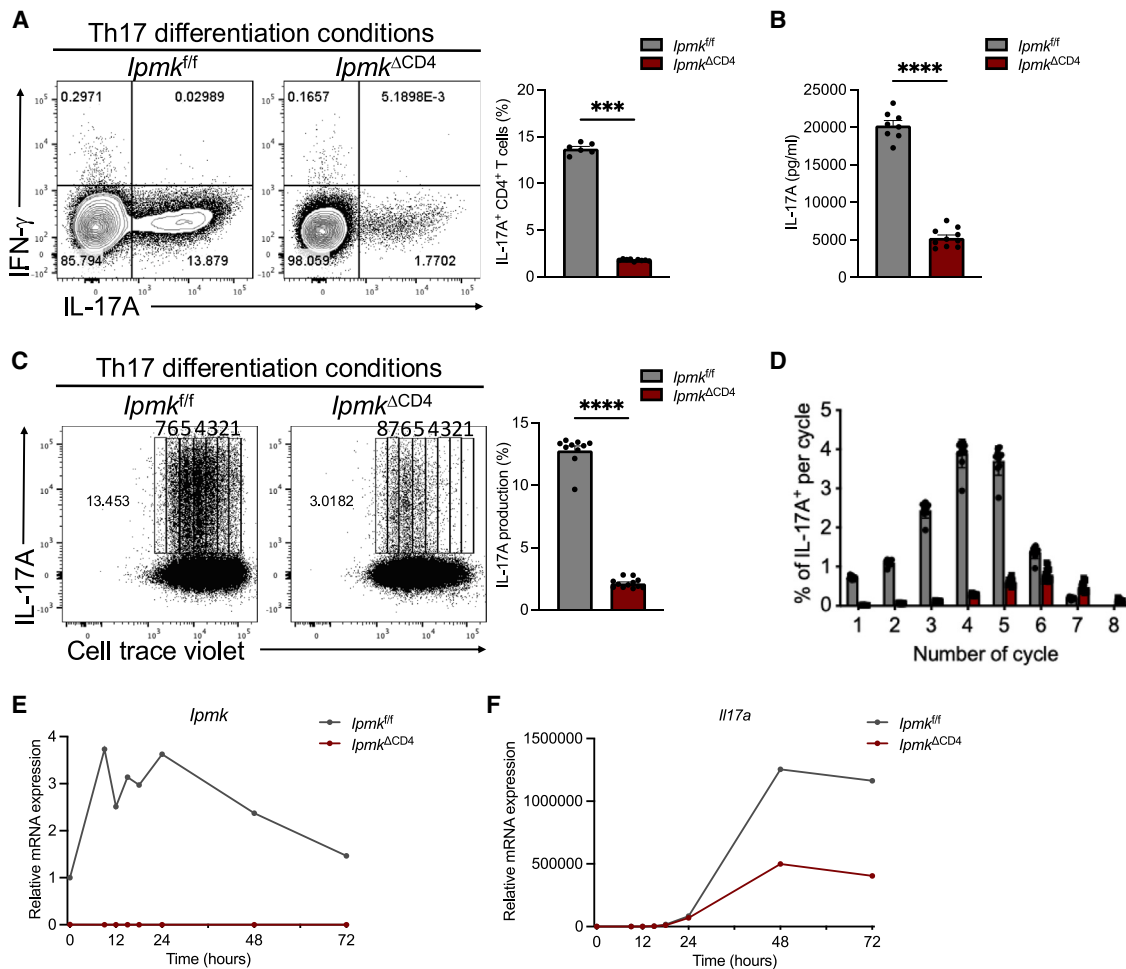


Figure 3. IPMK promotes Th17 cell differentiation

(A) Flow cytometry of IL-17A produced by Th17 cells from *lpmk*^{f/f} or *lpmk*^{ΔCD4} mice for 3 days *in vitro* ($n \geq 6$ per each group). (B) The IL-17A concentration of supernatant from Th17 cells culture conditions ($n \geq 8$ per each group). (C) The proliferation of Th17 cells of indicated genotypes over 3 days, assessed by CellTrace violet dilution assay and flow cytometry ($n \geq 10$ per group). (D) The percentage of IL-17⁺ cells at each cell proliferation cycle from 1 to 8, as shown in (C) of flow cytometry data. (E and F) Quantitative real-time PCR analysis of the time course of the expression of *lpmk* (E) and *l17a* (F) mRNA in naive CD4 T cells polarized into Th17 cells from *lpmk*^{f/f} or *lpmk*^{ΔCD4} mice.

Each image shows representative and compiling data. Data are presented as the mean \pm SEM; *** $p < 0.001$ and **** $p < 0.0001$ compared with the *lpmk*^{f/f} group by the Mann-Whitney test. See also Figure S1.

for the function of Th17 cells to mediate autoimmune pathology.

Next, to test the involvement of IPMK in Th2-mediated immune responses, we induced allergic asthma and analyzed the disease phenotypes and Th2 responses. For this, the *Aspergillus oryzae* protease (AP) mixed with chicken egg ovalbumin (OVA; APO) allergen^{24–26} was administrated, and asthma phenotypes, including airway hyperresponsiveness (AHR), recruitment of eosinophils, goblet cell metaplasia, and mucus hyperproduction, which are mediated by type 2 cytokines IL-4, IL-5, and IL-13, were examined.^{27–29} The APO allergen was intranasally administrated into *lpmk*^{f/f} and *lpmk*^{ΔCD4} mice five times, and allergic asthma symptoms were analyzed within 16 h of the final challenge (Figure S4A). Similar to WT controls, *lpmk*^{ΔCD4} mice

also showed enhanced symptoms of allergic asthma, including AHR, eosinophilic airway inflammation, mucus hyperproduction, and periodic acid-Schiff (PAS)-positive goblet cells, and increased secretion of type 2 cytokines (Figures S4B–S4I). Thus, these data indicate that IPMK is dispensable for the function of Th2 cells, as Th2-mediated immune responses were not affected. Collectively, IPMK-mediated signaling is important for the function of Th1 and Th17 cells but not Th2 cells.

IPMK is required for Th17 cell generation *in vitro*

Next, we investigated the effect of IPMK deficiency on *in vitro* T cell differentiation using naive CD4⁺ T cells from *lpmk*^{f/f} or *lpmk*^{ΔCD4} mice. In particular, we focused on Th17 cells, as they exhibit the most robust expression of IPMK (Figure S1) and

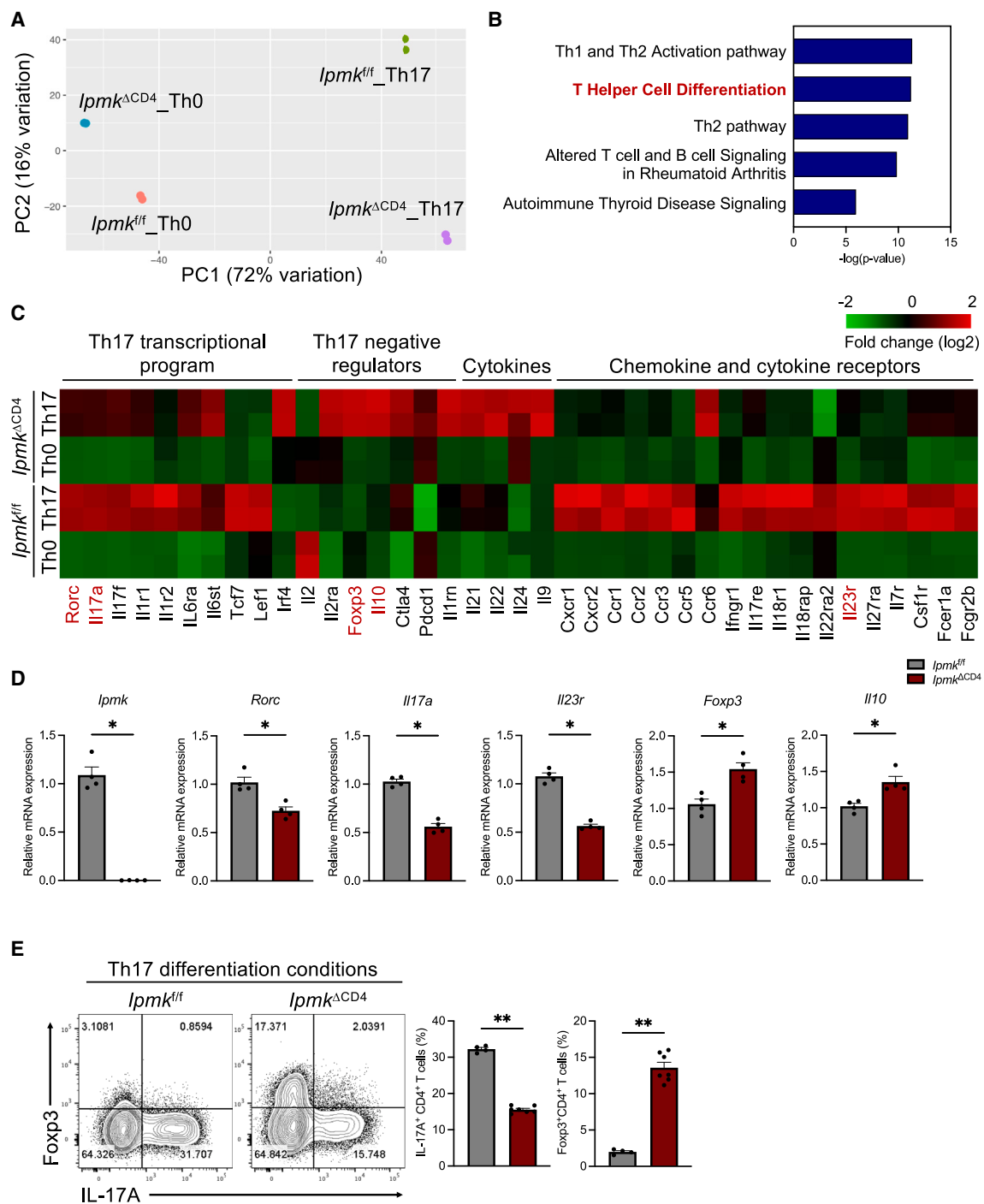


Figure 4. Transcriptionally distinct *lpmk^{f/f}* or *lpmk^{ΔCD4}* Th17 cells

(A) Principal-component analysis of the samples ($n = 2$).

(B) Pathway enrichment analysis of genes whose expression is significantly modulated by IPMK in Th17 cells from *lpmk^{f/f}* or *lpmk^{ΔCD4}* mice activated under indicated polarizing conditions for 3 days.

(C) Heatmap depicting the gene expression (FPKM) in the number of transcripts and red color significantly and differently expressed between *lpmk^{f/f}* or *lpmk^{ΔCD4}* cells stimulated indicated polarizing conditions. Data for each experimental group ($n = 2$ per condition) are shown. The color gradient indicates differentially expressed gene (DEG) expression as shown.

(legend continued on next page)

display severe *in vivo* defects in immune responses due to a deficiency in IPMK (Figure 2). Naive *lpmk^{ΔCD4}* CD4⁺ T cells displayed significant impairment in their differentiation into Th17 cells, as shown by a decrease in the IL-17A⁺ cell population compared to the *lpmk^{fl/fl}* CD4⁺ T cell population (Figure 3A) and diminished secretion of IL-17A into culture supernatants (Figure 3B). In addition, an analysis of the proliferation of *lpmk^{ΔCD4}* CD4⁺ T cells revealed a reduction in overall frequency (Figures 3C and 3D) and each proliferation cycle of IL-17A⁺ T cells (Figure 3D) compared to that of *lpmk^{fl/fl}* cells, suggesting that the impaired function of IPMK knockout (KO) Th17 cells is not merely a result of reduced proliferation. We also examined whether the kinetics of IPMK expression is dynamically changed under Th17-polarizing conditions and found the upregulation of *lpmk* mRNA 9 h after activation in the presence of IL-6 and TGF-β, which gradually diminished after 24 h (Figure 3E). In addition, the expression of *Il17a* was decreased in *lpmk^{ΔCD4}* T cells after 24 h under Th17 cell differentiation conditions (Figure 3F). Collectively, these findings strongly suggest that IPMK is a key factor for controlling the expression of IL-17A and generating functional Th17 cells.

IPMK globally regulates the transcriptional program of Th17 cells

Next, we performed genome-wide RNA sequencing (RNA-seq) analysis to assess the alteration of gene expression in IPMK-deficient cells during Th17 cell differentiation. Principal-component analysis (PCA) showed that *lpmk^{ΔCD4}* Th17 cells (*lpmk^{ΔCD4}_Th17*) were distinct from *lpmk^{fl/fl}* Th17 cells (*lpmk^{fl/fl}_Th17*). Furthermore, *lpmk^{ΔCD4}* Th0 cells (*lpmk^{ΔCD4}_Th0*) also differed from *lpmk^{fl/fl}* Th0 cells (*lpmk^{fl/fl}_Th0*) (Figure 4A). Gene Ontology analysis revealed that the Th cell differentiation pathway was modulated in *lpmk^{ΔCD4}* CD4 T cells differentiated into Th17 cells (Figure 4B). We next analyzed how IPMK deficiency affects the gene expression of Th17 cells and found that the expression of *Rorc*, *Il17a*, *Il17f*, *Il1r2*, *Tcf7*, and *Lef1*, genes related to Th17 transcriptional programs,^{30–32} was significantly decreased in *lpmk^{ΔCD4}* Th17 cells compared with *lpmk^{fl/fl}* Th17 cells. However, the expression of Th17 negative regulators *Il2ra*, *Foxp3*, and *Il10* was increased in *lpmk^{ΔCD4}* Th17 cells relative to *lpmk^{fl/fl}* Th17 cells (Figures 4 and S5). The validation of IPMK-related genes by reverse-transcription quantitative PCR (RT-qPCR) showed that *Rorc*, *IL17a*, and *IL23r*, which are hallmarks of Th17 cells, were upregulated in WT, but not IPMK-deficient, Th17 cells (Figure 4D). Moreover, we confirmed that the expression of *Foxp3*, a key regulator of Treg cell differentiation, and Treg-related cytokine *Il10* was increased in *lpmk^{ΔCD4}* naive CD4⁺ T cells stimulated under Th17-polarizing conditions compared to *lpmk^{fl/fl}* cells (Figure 4D). In addition to mRNA expression, *lpmk^{ΔCD4}* T cells displayed lower IL-17A, but higher Foxp3, protein expression than *lpmk^{fl/fl}* T cells during Th17 cell differentiation (Figure 4E). Thus, IPMK is required to encourage Th17 cell-related programs and restrict those of Treg cells during differentiation.

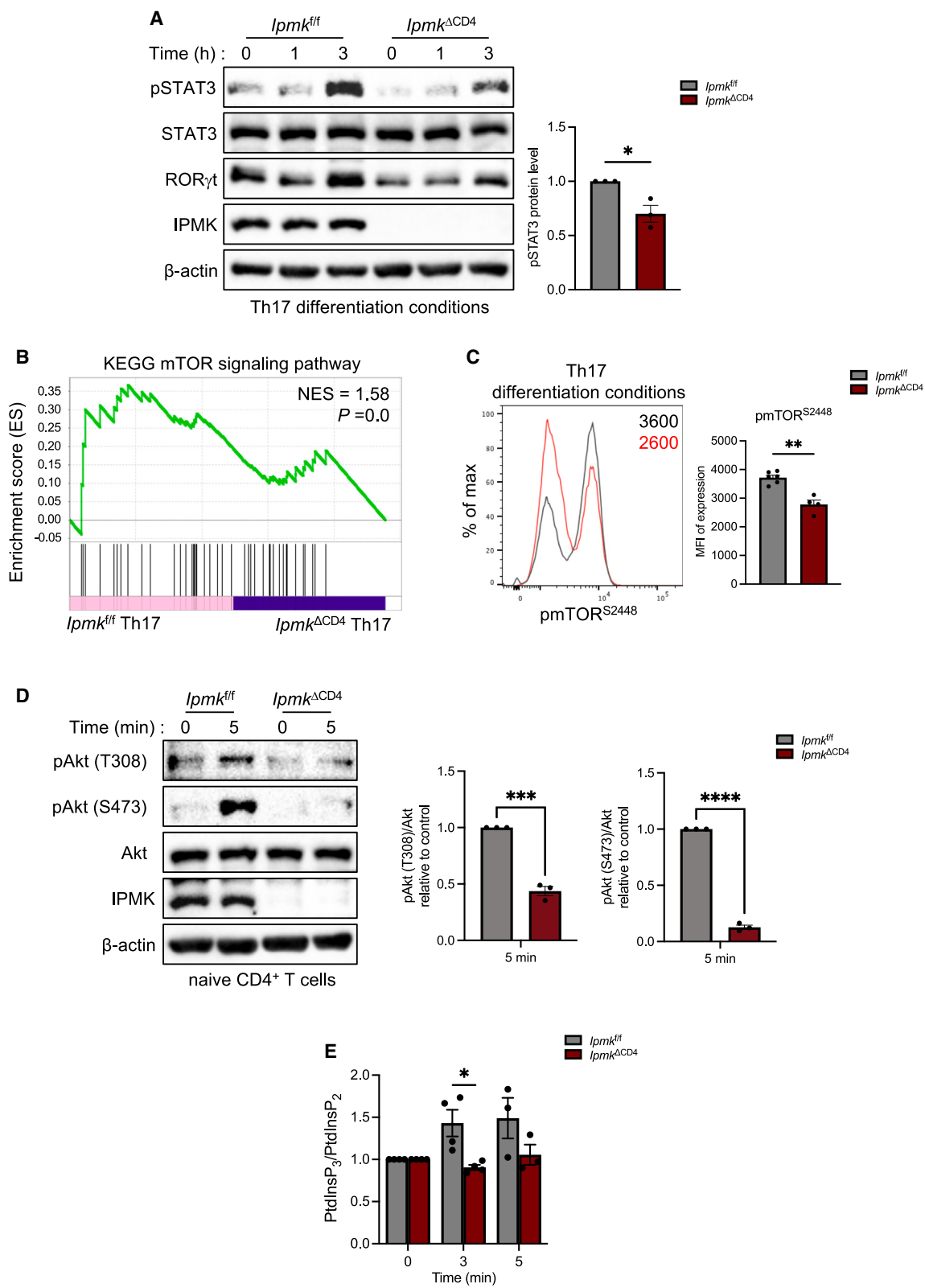
(D) Quantitative real-time PCR analysis to detect mRNA levels of Th17 cell-related genes and Treg cell-related genes expressed by CD4⁺ T cells of indicated genotypes activated under Th17 cell-polarizing conditions for 3 days (*n* = 4).

(E) Flow cytometry of IL-17A or Foxp3 expressed by nonpathogenic Th17 cell condition of *lpmk^{fl/fl}* or *lpmk^{ΔCD4}* cells for 3 days (*n* ≥ 4 per each group). Each image shows representative and compiling data. Data are presented as the mean ± SEM; **p* < 0.05 and ***p* < 0.01 compared with the *lpmk^{fl/fl}* group by the Mann-Whitney test. See also Figure S5.

IPMK is critical for STAT and Akt-mTOR signaling pathways in Th17 cells

Next, we further investigated the contribution of IPMK to the control of IL-6-mediated Th17 cell differentiation. STAT3 phosphorylation triggered by IL-6 is central to Th17 cell differentiation³³ and was found to be downregulated in *lpmk^{ΔCD4}* T cells during Th17 cell generation (Figure 5A). The phosphorylation of STAT3 Y705 and S727 residues is commonly regulated through Janus kinase 1 (JAK1), JAK2,³⁴ and mTORC1 during Th17 cell differentiation.³⁵ Accordingly, gene set enrichment analysis (GSEA) revealed that the mTOR signaling pathway was found to be downregulated in *lpmk^{ΔCD4}* Th17 cells (Figure 5B), and a reduction in phosphorylation of mTOR was seen in *lpmk^{ΔCD4}* Th17 cells (Figure 5C), suggesting a decrease in mTOR activation in the absence of IPMK. To address the association between the phosphorylation of STAT3 and mTOR activity, we examined whether Akt and mTOR activation was affected in *lpmk^{ΔCD4}* T cells. Diminished phosphorylation of Akt on both T308 and S473 residues was observed in *lpmk^{ΔCD4}* CD4⁺ T cells at early time points of TCR stimulation (Figures 5D, S6A, and S6B). Thus, this suggests that IPMK is required for the activation of Akt and mTOR signaling pathways in naive CD4⁺ T cells differentiated under Th17 cell conditions.

Next, we investigated the molecular mechanism of IPMK action in controlling Th17 differentiation and Akt signaling. In *lpmk^{ΔCD4}* CD4⁺ T cells, expression of the catalytically inactive IPMK-S235A mutant—which lacks both PI3K and InsP kinase activities—failed to stimulate Th17 differentiation, whereas WT IPMK expression increased the population of IL-17A⁺ cells (Figures S7A and S7B). In addition, expression of IPMK WT, but not IPMK-S235A, in naive *lpmk^{ΔCD4}* CD4⁺ T cells enhanced the phosphorylation of Akt on S473 in response to anti-CD3 and anti-CD28 antibodies (Figure S7C). These findings establish that IPMK's catalytic activities are essential for both Th17 differentiation and Akt activation. To further determine whether IPMK acts as an InsP kinase or PI3K, we measured the InsP profile and observed a decrease in higher-order InsPs, including InsP₄, InsP₅, InsP₆, and InsP₇ (Figure S8A), which are known to suppress Akt.³⁶ To test if supplementation with cell-permeable InsP could rescue the impaired Th17 differentiation, we treated *lpmk^{ΔCD4}* CD4⁺ T cells with cell-permeable InsP₄. This treatment failed to increase IL-17A⁺ cell levels (Figure S8B), suggesting that IPMK-dependent InsP synthesis is unrelated to Th17 differentiation. We then focused on IPMK's PI3K activity. To investigate whether IPMK expression in CD4⁺ T cells mediates Akt activation through controlling PIP₃ levels, we quantified PtdIns(4,5)P₂ and PtdIns(3,4,5)P₃ using liquid chromatography-mass spectrometry (LC-MS) based on derivatization³⁷ in naive CD4⁺ T cells. The ratio of PtdIns(3,4,5)P₃ to PtdIns(4,5)P₂ was decreased in *lpmk^{ΔCD4}* naive CD4⁺ T cells stimulated with anti-CD3 and anti-CD28 antibodies (Figure 5E). In the presence of wortmannin, a potent PI3K inhibitor, the ratio of PtdIns(3,4,5)P₃ to PtdIns(4,5)P₂ remained



(legend on next page)

suppressed at baseline levels in both WT and *Ipmk*^{ΔCD4} CD4⁺ T cells following stimulation with anti-CD3 and anti-CD28 antibodies (Figure S9A), suggesting the major contribution of IPMK to the production of PtdIns(3,4,5)P₃ in TCR-stimulated CD4⁺ T cells. We further examined the levels of the PI3Kδ, the primary classical PI3K isoform regulating T cell activation, Th17 differentiation, and autoimmunity, and observed no changes in *Ipmk*^{ΔCD4} T cells (Figure S9B). We next assessed the localization of IPMK in CD4⁺ T cells and found substantial amounts of endogenous IPMK in the membrane fractions from CD4⁺ T cells. The relative distribution of IPMK between membrane and cytoplasmic fractions remained unchanged in CD4⁺ T cells treated with anti-CD3 and anti-CD28 antibodies (Figure S9C), indicating a stable localization of IPMK with the plasma membrane in CD4⁺ T cells. To further validate the role of IPMK as a PI3K, we used the *Arabidopsis thaliana* ortholog of IPMK, Atlpk2β, which possesses only InsP kinase activity and lacks PI3K activity.¹⁸ In naive *Ipmk*^{ΔCD4} T cells, ectopic expression of WT IPMK stimulated the production of IL-17A⁺ cells, whereas Atlpk2β did not (Figure S10). Taken together, our findings support that the PI3K activity of IPMK is critical for generating PtdIns(3,4,5)P₃ in CD4⁺ T cells, which in turn activates the Akt-mTOR signaling pathway to drive Th17 cell differentiation.

IPMK-deficient CD4⁺ T cells exhibit an altered metabolic profile

In addition to STAT3 activation, mTOR has been shown to play an important role in the regulation of T cell metabolism through the activation of glycolysis-related genes.³⁸ Notably, T cell differentiation requires the activity of mTOR-dependent pathways, and in particular, the differentiation of Th1 and Th17 cells is induced through mTOR-dependent glycolysis. Therefore, we performed a mitochondrial stress test to assess mitochondrial respiration via the oxygen consumption rate (OCR) using the Seahorse extracellular flux analyzer. *Ipmk*^{ΔLck} T cells (Figure S2C) exhibited lower basal OCRs, maximal mitochondrial respiration, spare respiratory capacity, and ATP production than *Ipmk*^{t/t} CD4⁺ T cells (Figures 6A and 6B). We also assessed energy production through glycolysis using the XF glycolysis stress test. The basal extracellular acidification rate (ECAR), which correlates with lactate production by glycolysis, was reduced in *Ipmk*^{ΔLck} T cells but not *Ipmk*^{t/t} T cells. However, there were no differences in glycolytic capacity or glycolytic reserves between the two groups after the injection of an ATP

synthase inhibitor, oligomycin (Figures 6C and 6D). Consistently, we found that *Ipmk*^{ΔLck} T cells exhibited reduced OCRs and glycolytic energy production following the addition of oligomycin. Collectively, these results suggest that IPMK deficiency leads to impaired mitochondrial energy production and glycolysis in CD4⁺ T cells in a manner dependent on the STAT3-mTOR pathway.

DISCUSSION

In this study, we demonstrate that IPMK expression is elevated under Th1- and Th17-polarizing conditions but not Th2-polarizing conditions. To evaluate the role of IPMK in Th1 and Th17 cell functions, we used CD4⁺ T cell-specific genetic deletion of IPMK and found that the Th1 response was diminished as exhibited by enhanced susceptibility to *L. major* infection, which requires IFN-γ-dependent, Th1-mediated responses for clearance. Further, EAE, a Th17-dependent autoimmune disease model, exhibited delayed onset and a significantly attenuated Th17 response in *Ipmk*^{ΔCD4} mice. Moreover, IL-17A production was reduced in IPMK-deficient CD4⁺ T cells compared with WT CD4⁺ T cells under Th17-polarizing conditions. Mechanistically, we showed that IPMK participates in the cytokine signaling of STAT activation as a PI3K via the Akt-mTOR pathway, suggesting that IPMK is a critical regulator of Th1/Th17 cell differentiation (Figure 7).

IPMK is known to modulate various biological processes by working enzymatically to catalyze inositol polyphosphate biosynthesis^{39,40} and production of PIP₃¹⁸ and non-catalytically by regulating key signaling factors.^{20,41} For T cells, it is reported that IP₄ generated by ItpkB binds a single ITK subunit, causing its recruitment to the plasma membrane and resulting in the amplification of TCR signaling, triggering thymocyte positive selection.⁴² However, there are no reports as to whether IPMK has a role in CD4⁺ T cell differentiation and function. Therefore, we focused on IPMK in CD4⁺ Th cell differentiation, postulating that IPMK may be particularly important in both Th1 and Th17 responses and possibly Th1 or Th17 cell differentiation.

Upon activation, naive CD4⁺ T cells differentiate into effector T cells, including Th1, Th2, and Th17 cells, which regulate immunity against various pathogens differently. These effector T cells are differentially induced by distinct environmental cytokines, which signal through STATs or ubiquitous and other inducible transcription factors.⁴³ Interestingly, both IPMK protein and

Figure 5. Defective activation of the Akt-mTOR pathway in *Ipmk*^{ΔCD4} CD4⁺ T cells

- (A) Immunoblotting of STAT3 phosphorylated at Y705 or total STAT3 in lysates of naive CD4⁺ T cells polarized for 3 days under Th17 conditions from *Ipmk*^{t/t} or *Ipmk*^{ΔCD4} and then restimulated for various times with IL-6 and TGF-β. Unpaired Student's t test was used for statistical analysis; *p < 0.05 compared with the *Ipmk*^{t/t} group.
- (B) GSEA-based KEGG enrichment plots for downregulated genes in mTOR signaling pathway of *Ipmk*^{ΔCD4} Th17 cells.
- (C) Sorted naive CD4⁺ T cells were differentiated under Th17 conditions and evaluated for levels of p-mTOR (S2448). **p < 0.01 compared with the *Ipmk*^{t/t} group by the Mann-Whitney test.
- (D) Immunoblotting of AKT phosphorylated at T308, S473, and total AKT in lysates of naive CD4⁺ T cells stimulated with anti-CD3, anti-CD28, and anti-hamster immunoglobulin (Ig)G antibodies. Unpaired two-tailed Student's t test was used for statistical analysis; ***p < 0.001; ****p < 0.0001 compared with the *Ipmk*^{t/t} group.
- (E) Measuring the ratio of PtdInsP₃ to PtdInsP₂ in naive *Ipmk*^{t/t} or *Ipmk*^{ΔCD4} CD4⁺ T cells, which were stimulated with anti-CD3, anti-CD28, and anti-hamster IgG antibodies. PtdInsP₃ and PtdInsP₂ levels were quantified by LC-tandem MS (LC-MS/MS; technical replicates n = 4). *p < 0.05 compared with the *Ipmk*^{t/t} group by the Mann-Whitney test.

Each image shows representative and compiling data. Data are presented as the mean ± SEM. See also Figures S6–S10.

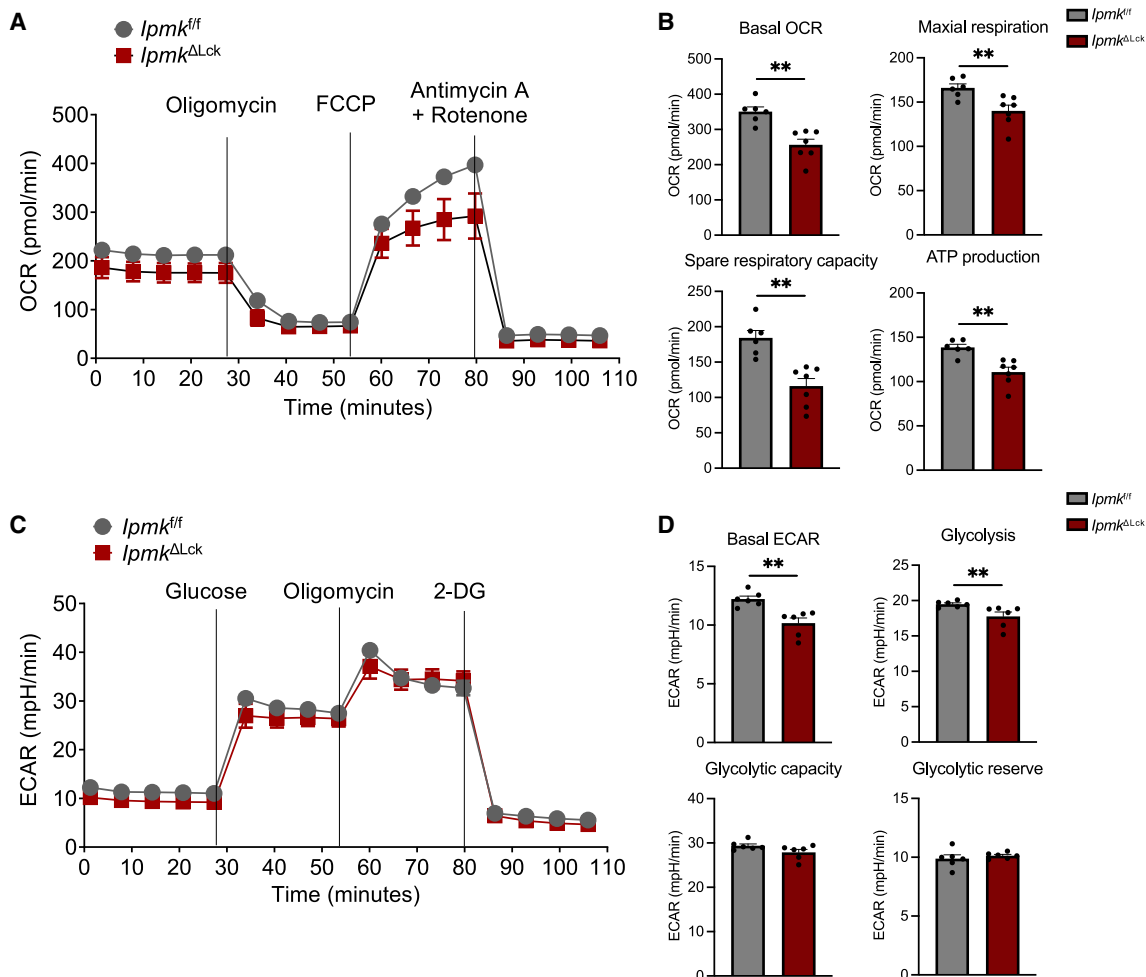


Figure 6. Reduced aerobic glycolysis and mitochondrial oxidative respiration with IPMK in CD4⁺ T cells

(A–D) CD4 cells from *Ipmk^{f/f}* or *Ipmk^{ΔLck}* were activated with Dynabeads for 72 h.

(A and B) OCR (A) was measured by Seahorse XFe Analyzer and basal OCR, maximal respiration, spare respiratory capacity, and ATP production (B) were calculated.

(C and D) ECAR (C) was measured by Seahorse XFe Analyzer and basal ECAR, glycolysis, glycolytic capacity, and glycolytic reserve (D) were calculated.

Each image shows representative and compiling data. Data are presented as the mean ± SEM; ***p* < 0.01 compared with the *Ipmk^{f/f}* group by the Mann-Whitney test.

transcripts increased in Th17 cells. In addition, *Ipmk^{ΔCD4}* T cells cannot be differentiated into Th17 cells, showing attenuated production of IL-17A relative to that of *Ipmk^{f/f}* Th17 cells. Differentiation of Th17 cells requires a variety of transcription factors, such as STAT3, ROR γ T, Ahr, BATF, IRF4, etc.^{44–46} Genome-wide sequencing analyses revealed that under Th17-polarizing conditions, *Ipmk^{ΔCD4}* T cells show decreased *Il17a*, *Rorc*, and *Il23r* transcription. Surprisingly, expression of Foxp3, a master transcription factor for Treg cells,⁴⁷ was the most upregulated gene in *Ipmk^{ΔCD4}* Th17 cells. Foxp3⁺ Treg cells are critical for maintaining immune tolerance and controlling immune responses toward pathogens. Interestingly, Th17 and Treg cells are closely related and reciprocally regulated, as they share TGF- β cytokine signaling. Therefore, our findings propose IPMK as the key factor to balance Th17 and Treg cell development critical for host protective immunity.

During T cell activation, ligation of receptors by costimulatory molecules induces PI3K activation and consequently activates mTOR, which induces the differentiation of effector T cells. The two mTOR complexes, mTORC1 and mTORC2, have disparate effects on effector T cell differentiation.^{48,49} *Rheb*-deficient CD4⁺ T cells exhibit selectively abrogated tyrosine phosphorylation of STAT3 and STAT4, which is a result of increased suppressor of cytokine signaling 3 (SOCS3) protein expression.¹⁵ The mTOR-deficient T cells are unable to activate lineage-specific STAT proteins and major transcription factors. *Rheb* protein deficiency and the consequent loss of mTORC1 activity lead to the impaired differentiation of Th1 and Th17 cells. Thus, this suggests that mTORC1 mediates the mTOR-dependent differentiation of Th1 and Th17 cells. The findings in the present study suggest that through its PI3K activity, IPMK is a key factor mediating the full activation of Akt-mTOR signaling. Specifically, this

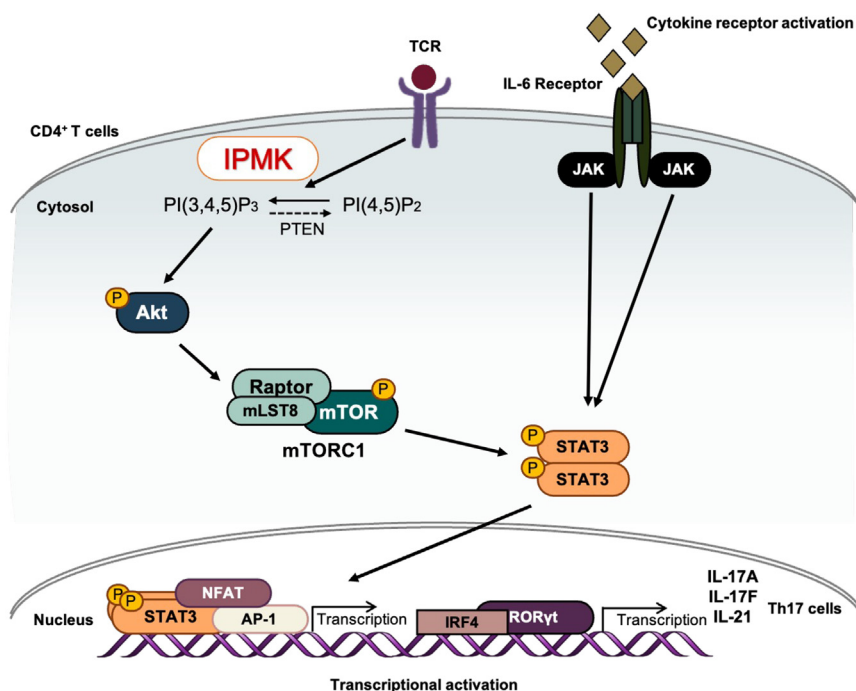


Figure 7. A model deciphering action of IPMK in CD4 T cells under Th17 differentiation condition

Graphic abstract showing how CD4 IPMK signaling regulates Th17 cell differentiation. IPMK activation by IL-6 and TCR signaling causes Akt-mTORC1 and STAT3 phosphorylation. These changes collectively induce Th17 differentiation.

role is evidenced by the reduced PIP₃ generation in *lpmk*^{ΔCD4} T cells. Th17 differentiation and Akt signaling require the PI3K activity of IPMK, as neither a kinase-dead mutant nor Atlpk2β elicits an effect. In activated T cells, class I PI3K p110δ has been shown to be a primary enzyme involved in the generation of PIP₃, thus governing proliferation, cytokine production, and differentiation into Th subsets.^{10,50–52} Although IPMK exhibits robust wortmannin-insensitive PI3K activity *in vitro* and IPMK depletion in cell lines (e.g., heterologous MEFs and cancer cells) reduces growth-factor-stimulated PIP₃ synthesis accompanied by hypoactivation of Akt-mTOR signaling,⁵³ it was challenging to elucidate the appropriate physiological context in which IPMK's PI3K activity fulfills a central role in Akt-mTOR activation. In the present study, we identify that IPMK remains stably associated with the plasma membrane in the absence or presence of TCR stimulation in CD4⁺ T cells. In both *lpmk*^{f/f} and *lpmk*^{ΔCD4} CD4⁺ T cells, the levels of PIP₃ generation upon TCR stimulation are virtually abolished following wortmannin treatment, suggesting that IPMK acts as a PI3K in a wortmannin-sensitive manner. A previous study proposes that phosphorylation on IPMK in response to growth factor receptor stimulation may be required to switch on its PI3K activity in cells.¹⁸ Future investigations are needed to elucidate the precise mechanisms by which IPMK in Th cells collaborates with other wortmannin-sensitive PI3Ks, such as p110δ, to synthesize PIP₃, enhance Akt signaling, and trigger cellular responses involved in T cell activation and differentiation.

The signaling actions of IPMK in immune cells seem to vary widely depending on the specific cell type. In B cells, IPMK's catalytic action in water-soluble inositol polyphosphate biosynthesis is critical for lipopolysaccharide (LPS)-triggered B cell receptor signaling via InsP₆-dependent Btk activation.²¹ In mac-

rophages, IPMK seems to non-catalytically function as a scaffold to stabilize TRAF6 and transmit TLR4 signals.²⁰ Recently, conditional deletion of IPMK in Treg cells revealed its essential role for the regulatory function and differentiation of Treg cells into effector Treg cells. Mechanistically, IPMK's catalytic activity as an IP kinase was found to promote InsP₃-mediated store-operated Ca²⁺ entry (SOCE) via InsP₄ (Ins(1,3,4,5)P₄) production in Treg cells.⁵⁴ In contrast, our results in the present study revealed that Th cells depend on the lipid PI3K function of IPMK to regulate activation of mTOR signaling, which directly modulates

STAT3 activation and governs Th1 and Th17 cell differentiation. Future studies are needed to define the signaling mechanisms by which IPMK in Th cells cooperates with other classical PI3Ks, such as P110δ, to fully mediate T cell activation, differentiation, and homeostasis. The recent discovery of SNPs in IPMK in immune-mediated diseases (e.g., rheumatoid arthritis, psoriasis, and Crohn's disease) further highlights the possible contribution of IPMK to the onset and progress of Th cell-mediated human diseases.¹⁹

In summary, our study explores the role of IPMK in proinflammatory CD4⁺ T cell function. Moreover, deletion of IPMK in CD4⁺ T cells attenuates resistance to *L. major* infection and the severity of EAE by impairing Th1 and Th17 cell differentiation. Given the vital importance of Th1 and Th17 cells in T cell immunity, we suggest that regulation of IPMK in CD4⁺ Th cells could be beneficial for the treatment of infections as well as autoimmune disorders.

Limitations of the study

Although we demonstrated IPMK's physiological function as a PI3K in Th1 and Th17 immunity, a deeper understanding of the biochemical mechanisms governing IPMK's catalytic activation and inactivation during T cell activation is necessary. Further studies are also required to determine whether IPMK directly modulates the activity and function of classical PI3Ks, such as p110δ. Additionally, it will be important to investigate whether IPMK influences other Th subtypes, such as follicular Th (Tfh) cells.

RESOURCE AVAILABILITY

Lead contact

Requests for further information and resources should be directed to and will be fulfilled by the lead contact, Seung-Hyo Lee (s131345@kaist.ac.kr).

Materials availability

Materials generated in this study are available upon request from the lead contact.

Data and code availability

- The RNA-seq data generated in this study have been deposited in the Gene Expression Omnibus (GEO) database (GEO: GSE203137) and are publicly accessible.
- This paper does not report original code.
- Additional information needed to reanalyze the reported data is available upon request from the lead contact.

ACKNOWLEDGMENTS

We thank Dr. Hyunji Lee for technical assistance and the Hyewha Forum and Dr. Suk-Jo Kang for helpful discussions. This study was supported by grants funded by the Korea Mouse Phenotyping Project (NRF-2014M3A9D5A01073789 to R.H.S.), the National Research Foundation of Korea (NRF-2018R1A5A1024261, NRF-2020R1A2C3005765, RS-2023-00278918, and RS-2024-00415888 to S.K.), the Samsung Science & Technology Foundation (SSTF-BA1401-14 to S.K.), and the Biomlogic/GenoFocus (to S.-H.L.).

AUTHOR CONTRIBUTIONS

C.M.Y., S.H., D.K., R.H.S., S.K., and S.-H.L. conceived the project and designed the experiments. C.M.Y., S.H., D.K., S.K., and S.-H.L. performed most of the experiments, interpreted the data, and contributed to the discussion of the results. M.K., S.J.P., H.M., and W.K. assisted with *in vivo* experiments and provided advice. H.-W.J. supported RNA-seq data analysis and discussions. J.L. and S.-G.K. aided in quantifying PtdInsP(3,4,5)₃/PtdInsP(4,5)₂ and discussions. H.D.K. helped with CD4⁺ T cell membrane and cytoplasm fractionation. C.M.Y., S.H., D.K., M.K., S.K., and S.-H.L. wrote the manuscript. R.H.S., S.K., and S.-H.L. supervised the experiments and discussions. S.-H.L. held final responsibility for submission.

DECLARATION OF INTERESTS

The authors declare no competing interests.

STAR METHODS

Detailed methods are provided in the online version of this paper and include the following:

- KEY RESOURCES TABLE
- EXPERIMENTAL MODEL AND STUDY PARTICIPANT DETAILS
 - Mice
- METHOD DETAILS
 - CD4⁺ T cell differentiation and proliferation *in vitro*
 - Viral transduction into CD4⁺ T cells
 - Western blot analysis
 - Flow cytometry
 - *Leishmania major* parasites and infectious challenge
 - Intracellular cytokine staining (ICCS)
 - EAE model
 - Induction of experimental allergic asthma
 - Measurement of airway hyperresponsiveness (AHR)
 - Quantification of secreted glycoprotein
 - ELISA for cytokine detection
 - Lung tissue histology
 - RNA isolation and quantitative RT-PCR
 - RNA sequencing
 - Cytometric bead array (CBA)
 - Quantification of inositol polyphosphates
 - Quantification of PtdInsP(3,4,5)₃/PtdInsP(4,5)₂
 - Mitochondrial respiration and glycolysis assay
- QUANTIFICATION AND STATISTICAL ANALYSIS

SUPPLEMENTAL INFORMATION

Supplemental information can be found online at <https://doi.org/10.1016/j.celrep.2025.115281>.

Received: August 8, 2023

Revised: November 15, 2024

Accepted: January 16, 2025

Published: February 12, 2025

REFERENCES

1. Luckheeram, R.V., Zhou, R., Verma, A.D., and Xia, B. (2012). CD4(+)-T cells: differentiation and functions. *Clin. Dev. Immunol.* 2012, 925135. <https://doi.org/10.1155/2012/925135>.
2. Dong, C. (2008). TH17 cells in development: an updated view of their molecular identity and genetic programming. *Nat. Rev. Immunol.* 8, 337–348. <https://doi.org/10.1038/nri2295>.
3. Zou, W., and Restifo, N.P. (2010). T(H)17 cells in tumour immunity and immunotherapy. *Nat. Rev. Immunol.* 10, 248–256. <https://doi.org/10.1038/nri2742>.
4. Peters, A., Lee, Y., and Kuchroo, V.K. (2011). The many faces of Th17 cells. *Curr. Opin. Immunol.* 23, 702–706. <https://doi.org/10.1016/j.coim.2011.08.007>.
5. Korn, T., Bettelli, E., Oukka, M., and Kuchroo, V.K. (2009). IL-17 and Th17 Cells. *Annu. Rev. Immunol.* 27, 485–517. <https://doi.org/10.1146/annurev.immunol.021908.132710>.
6. Durant, L., Watford, W.T., Ramos, H.L., Laurence, A., Vahedi, G., Wei, L., Takahashi, H., Sun, H.W., Kanno, Y., Powrie, F., and O'Shea, J.J. (2010). Diverse targets of the transcription factor STAT3 contribute to T cell pathogenicity and homeostasis. *Immunity* 32, 605–615. <https://doi.org/10.1016/j.jimmuni.2010.05.003>.
7. Fossiez, F., Djossou, O., Chomarat, P., Flores-Romo, L., Ait-Yahia, S., Maat, C., Pin, J.J., Garrone, P., Garcia, E., Saeland, S., et al. (1996). T cell interleukin-17 induces stromal cells to produce proinflammatory and hematopoietic cytokines. *J. Exp. Med.* 183, 2593–2603. <https://doi.org/10.1084/jem.183.6.2593>.
8. Tan, W., Huang, W., Zhong, Q., and Schwarzenberger, P. (2006). IL-17 receptor knockout mice have enhanced myelotoxicity and impaired hematopoietic recovery following gamma irradiation. *J. Immunol.* 176, 6186–6193. <https://doi.org/10.4049/jimmunol.176.10.6186>.
9. Kane, L.P., and Weiss, A. (2003). The PI-3 kinase/Akt pathway and T cell activation: pleiotropic pathways downstream of PIP3. *Immunol. Rev.* 192, 7–20. <https://doi.org/10.1034/j.1600-065x.2003.00008.x>.
10. Huang, Y.H., and Sauer, K. (2010). Lipid signaling in T-cell development and function. *Cold Spring Harb. Perspect. Biol.* 2, a002428. <https://doi.org/10.1101/cshperspect.a002428>.
11. Kurebayashi, Y., Nagai, S., Ikejiri, A., Ohtani, M., Ichiyama, K., Baba, Y., Yamada, T., Egami, S., Hoshii, T., Hirao, A., et al. (2012). PI3K-Akt-mTORC1-S6K1/2 axis controls Th17 differentiation by regulating Gfi1 expression and nuclear translocation of ROR γ . *Cell Rep.* 1, 360–373. <https://doi.org/10.1016/j.celrep.2012.02.007>.
12. Shi, L.Z., Wang, R., Huang, G., Vogel, P., Neale, G., Green, D.R., and Chi, H. (2011). HIF1alpha-dependent glycolytic pathway orchestrates a metabolic checkpoint for the differentiation of TH17 and Treg cells. *J. Exp. Med.* 208, 1367–1376. <https://doi.org/10.1084/jem.20110278>.
13. Ikejiri, A., Nagai, S., Goda, N., Kurebayashi, Y., Osada-Oka, M., Takubo, K., Suda, T., and Koyasu, S. (2012). Dynamic regulation of Th17 differentiation by oxygen concentrations. *Int. Immunol.* 24, 137–146. <https://doi.org/10.1093/intimm/dxr111>.
14. Dang, E.V., Barbi, J., Yang, H.Y., Jinasena, D., Yu, H., Zheng, Y., Bordman, Z., Fu, J., Kim, Y., Yen, H.R., et al. (2011). Control of T(H)17/T(reg) balance by hypoxia-inducible factor 1. *Cell* 146, 772–784. <https://doi.org/10.1016/j.cell.2011.07.033>.

15. Delgoffe, G.M., Polizzi, K.N., Waickman, A.T., Heikamp, E., Meyers, D.J., Horton, M.R., Xiao, B., Worley, P.F., and Powell, J.D. (2011). The kinase mTOR regulates the differentiation of helper T cells through the selective activation of signaling by mTORC1 and mTORC2. *Nat. Immunol.* 12, 295–303. <https://doi.org/10.1038/ni.2005>.
16. Kim, S., Bhandari, R., Brearley, C.A., and Saiardi, A. (2024). The inositol phosphate signalling network in physiology and disease. *Trends Biochem. Sci.* 49, 969–985. <https://doi.org/10.1016/j.tibs.2024.08.005>.
17. Resnick, A.C., Snowman, A.M., Kang, B.N., Hurt, K.J., Snyder, S.H., and Saiardi, A. (2005). Inositol polyphosphate multikinase is a nuclear PI3-kinase with transcriptional regulatory activity. *Proc. Natl. Acad. Sci. USA* 102, 12783–12788. <https://doi.org/10.1073/pnas.0506184102>.
18. Maag, D., Maxwell, M.J., Hardesty, D.A., Boucher, K.L., Choudhari, N., Hanno, A.G., Ma, J.F., Snowman, A.S., Pietropaoli, J.W., Xu, R., et al. (2011). Inositol polyphosphate multikinase is a physiologic PI3-kinase that activates Akt/PKB. *Proc. Natl. Acad. Sci. USA* 108, 1391–1396. <https://doi.org/10.1073/pnas.1017831108>.
19. Yokoyama, J.S., Wang, Y., Schork, A.J., Thompson, W.K., Karch, C.M., Cruchaga, C., McEvoy, L.K., Witkoelar, A., Chen, C.H., Holland, D., et al. (2016). Association Between Genetic Traits for Immune-Mediated Diseases and Alzheimer Disease. *JAMA Neurol.* 73, 691–697. <https://doi.org/10.1001/jamaneurol.2016.0150>.
20. Kim, E., Beon, J., Lee, S., Park, S.J., Ahn, H., Kim, M.G., Park, J.E., Kim, W., Yuk, J.M., Kang, S.J., et al. (2017). Inositol polyphosphate multikinase promotes Toll-like receptor-induced inflammation by stabilizing TRAF6. *Sci. Adv.* 3, e1602296. <https://doi.org/10.1126/sciadv.1602296>.
21. Kim, W., Kim, E., Min, H., Kim, M.G., Eisenbeis, V.B., Dutta, A.K., Pavlovic, I., Jessen, H.J., Kim, S., and Seong, R.H. (2019). Inositol polyphosphates promote T cell-independent humoral immunity via the regulation of Bruton's tyrosine kinase. *Proc. Natl. Acad. Sci. USA* 116, 12952–12957. <https://doi.org/10.1073/pnas.1821552116>.
22. Sacks, D., and Noben-Trauth, N. (2002). The immunology of susceptibility and resistance to Leishmania major in mice. *Nat. Rev. Immunol.* 2, 845–858. <https://doi.org/10.1038/nri933>.
23. Scott, P., Natovitz, P., Coffman, R.L., Pearce, E., and Sher, A. (1988). Immunoregulation of cutaneous leishmaniasis. T cell lines that transfer protective immunity or exacerbation belong to different T helper subsets and respond to distinct parasite antigens. *J. Exp. Med.* 168, 1675–1684. <https://doi.org/10.1084/jem.168.5.1675>.
24. Kwon, B.I., Kim, T.W., Shin, K., Kim, Y.H., Yuk, C.M., Yuk, J.M., Shin, D.M., Jo, E.K., Lee, C.H., and Lee, S.H. (2017). Enhanced Th2 cell differentiation and function in the absence of Nox2. *Allergy* 72, 252–265. <https://doi.org/10.1111/all.12944>.
25. Kim, Y.H., Kim, D.E., and Lee, S.H. (2018). Effects of 18beta-Glycyrheticin Acid on Fungal Protease-Induced Airway Inflammatory Responses. *Meditators Inflamm.* 2018, 6461032. <https://doi.org/10.1155/2018/6461032>.
26. Kim, D.E., Lee, Y., Kim, M., Lee, S., Jon, S., and Lee, S.H. (2017). Bilirubin nanoparticles ameliorate allergic lung inflammation in a mouse model of asthma. *Biomaterials* 140, 37–44. <https://doi.org/10.1016/j.biomaterials.2017.06.014>.
27. Walker, J.A., and McKenzie, A.N.J. (2018). TH2 cell development and function. *Nat. Rev. Immunol.* 18, 121–133. <https://doi.org/10.1038/nri.2017.118>.
28. Leon, B., and Ballesteros-Tato, A. (2021). Modulating Th2 Cell Immunity for the Treatment of Asthma. *Front. Immunol.* 12, 637948. <https://doi.org/10.3389/fimmu.2021.637948>.
29. Lambrecht, B.N., and Hammad, H. (2015). The immunology of asthma. *Nat. Immunol.* 16, 45–56. <https://doi.org/10.1038/ni.3049>.
30. Crome, S.Q., Wang, A.Y., and Levings, M.K. (2010). Translational mini-review series on Th17 cells: function and regulation of human T helper 17 cells in health and disease. *Clin. Exp. Immunol.* 159, 109–119. <https://doi.org/10.1111/j.1365-2249.2009.04037.x>.
31. Yu, Q., Sharma, A., Ghosh, A., and Sen, J.M. (2011). T cell factor-1 negatively regulates expression of IL-17 family of cytokines and protects mice from experimental autoimmune encephalomyelitis. *J. Immunol.* 186, 3946–3952. <https://doi.org/10.4049/jimmunol.1003497>.
32. Muranski, P., Borman, Z.A., Kerkar, S.P., Klebanoff, C.A., Ji, Y., Sanchez-Perez, L., Sukumar, M., Reger, R.N., Yu, Z., Kern, S.J., et al. (2011). Th17 cells are long lived and retain a stem cell-like molecular signature. *Immunity* 35, 972–985. <https://doi.org/10.1016/j.immuni.2011.09.019>.
33. Yang, X.O., Panopoulos, A.D., Nurieva, R., Chang, S.H., Wang, D., Watowich, S.S., and Dong, C. (2007). STAT3 regulates cytokine-mediated generation of inflammatory helper T cells. *J. Biol. Chem.* 282, 9358–9363. <https://doi.org/10.1074/jbc.C600321200>.
34. Seif, F., Khoshmirsafa, M., Aazami, H., Mohsenzadegan, M., Sedighi, G., and Bahar, M. (2017). The role of JAK-STAT signaling pathway and its regulators in the fate of T helper cells. *Cell Commun. Signal.* 15, 23. <https://doi.org/10.1186/s12964-017-0177-y>.
35. Bezzerra, V., Vella, A., Calcaterra, E., Finotti, A., Gasparello, J., Gambari, R., Assael, B.M., Cipolli, M., and Sorio, C. (2016). New insights into the Shwachman-Diamond Syndrome-related haematological disorder: hyper-activation of mTOR and STAT3 in leukocytes. *Sci. Rep.* 6, 33165. <https://doi.org/10.1038/srep33165>.
36. Chakraborty, A., Kim, S., and Snyder, S.H. (2011). Inositol pyrophosphates as mammalian cell signals. *Sci. Signal.* 4, re1. <https://doi.org/10.1126/scisignal.2001958>.
37. Clark, J., Anderson, K.E., Juvvin, V., Smith, T.S., Karpe, F., Wakelam, M.J.O., Stephens, L.R., and Hawkins, P.T. (2011). Quantification of PtlnsP3 molecular species in cells and tissues by mass spectrometry. *Nat. Methods* 8, 267–272. <https://doi.org/10.1038/nmeth.1564>.
38. Linke, M., Fritsch, S.D., Sukhbaatar, N., Hengstschläger, M., and Weichhart, T. (2017). mTORC1 and mTORC2 as regulators of cell metabolism in immunity. *FEBS Lett.* 591, 3089–3103. <https://doi.org/10.1002/1873-3468.12711>.
39. Saiardi, A., Erdjument-Bromage, H., Snowman, A.M., Tempst, P., and Snyder, S.H. (1999). Synthesis of diphosphoinositol pentakisphosphate by a newly identified family of higher inositol polyphosphate kinases. *Curr. Biol.* 9, 1323–1326. [https://doi.org/10.1016/s0960-9822\(00\)80055-x](https://doi.org/10.1016/s0960-9822(00)80055-x).
40. Odom, A.R., Stahlberg, A., Wente, S.R., and York, J.D. (2000). A role for nuclear inositol 1,4,5-trisphosphate kinase in transcriptional control. *Science* 287, 2026–2029. <https://doi.org/10.1126/science.287.5460.2026>.
41. Kim, S., Kim, S.F., Maag, D., Maxwell, M.J., Resnick, A.C., Juluri, K.R., Chakraborty, A., Koldobskiy, M.A., Cha, S.H., Barrow, R., et al. (2011). Amino acid signaling to mTOR mediated by inositol polyphosphate multikinase. *Cell Metab.* 13, 215–221. <https://doi.org/10.1016/j.cmet.2011.01.007>.
42. Huang, Y.H., Grasis, J.A., Miller, A.T., Xu, R., Soonthornvacharin, S., Andreotti, A.H., Tsoukas, C.D., Cooke, M.P., and Sauer, K. (2007). Positive regulation of Itk PH domain function by soluble IP4. *Science* 316, 886–889. <https://doi.org/10.1126/science.1138684>.
43. Zhu, J., Yamane, H., and Paul, W.E. (2010). Differentiation of effector CD4 T cell populations (*). *Annu. Rev. Immunol.* 28, 445–489. <https://doi.org/10.1146/annurev-immunol-030409-101212>.
44. Dong, C. (2011). Genetic controls of Th17 cell differentiation and plasticity. *Exp. Mol. Med.* 43, 1–6. <https://doi.org/10.3858/emm.2011.43.1.007>.
45. Yosef, N., Shalek, A.K., Gaublomme, J.T., Jin, H., Lee, Y., Awasthi, A., Wu, C., Karwacz, K., Xiao, S., Jorgoll, M., et al. (2013). Dynamic regulatory network controlling Th17 cell differentiation. *Nature* 496, 461–468. <https://doi.org/10.1038/nature11981>.
46. Ciofani, M., Madar, A., Galan, C., Sellars, M., Mace, K., Pauli, F., Agarwal, A., Huang, W., Parkhurst, C.N., Muratet, M., et al. (2012). A validated regulatory network for Th17 cell specification. *Cell* 151, 289–303. <https://doi.org/10.1016/j.cell.2012.09.016>.

47. Li, Z., Li, D., Tsun, A., and Li, B. (2015). FOXP3+ regulatory T cells and their functional regulation. *Cell. Mol. Immunol.* 12, 558–565. <https://doi.org/10.1038/cmi.2015.10>.
48. Delgoffe, G.M., Kole, T.P., Zheng, Y., Zarek, P.E., Matthews, K.L., Xiao, B., Worley, P.F., Kozma, S.C., and Powell, J.D. (2009). The mTOR kinase differentially regulates effector and regulatory T cell lineage commitment. *Immunity* 30, 832–844. <https://doi.org/10.1016/j.immuni.2009.04.014>.
49. Chi, H. (2012). Regulation and function of mTOR signalling in T cell fate decisions. *Nat. Rev. Immunol.* 12, 325–338. <https://doi.org/10.1038/nri3198>.
50. Okkenhaug, K., Bilancio, A., Farjot, G., Priddle, H., Sancho, S., Peskett, E., Pearce, W., Meek, S.E., Salpekar, A., Waterfield, M.D., et al. (2002). Impaired B and T cell antigen receptor signaling in p110delta PI 3-kinase mutant mice. *Science* 297, 1031–1034. <https://doi.org/10.1126/science.1073560>.
51. Okkenhaug, K., Patton, D.T., Bilancio, A., Garçon, F., Rowan, W.C., and Vanhaesebroeck, B. (2006). The p110delta isoform of phosphoinositide 3-kinase controls clonal expansion and differentiation of Th cells. *J. Immunol.* 177, 5122–5128. <https://doi.org/10.4049/jimmunol.177.8.5122>.
52. Sinclair, L.V., Finlay, D., Feijoo, C., Cornish, G.H., Gray, A., Ager, A., Okkenhaug, K., Hagenbeek, T.J., Spits, H., and Cantrell, D.A. (2008). Phosphatidylinositol-3-OH kinase and nutrient-sensing mTOR pathways control T lymphocyte trafficking. *Nat. Immunol.* 9, 513–521. <https://doi.org/10.1038/ni.1603>.
53. Reilly, L., Semenza, E.R., Koshkaryan, G., Mishra, S., Chatterjee, S., Abramson, E., Mishra, P., Sei, Y., Wank, S.A., Donowitz, M., et al. (2023). Loss of PI3k activity of inositol polyphosphate multikinase impairs PDK1-mediated AKT activation, cell migration, and intestinal homeostasis. *iScience* 26, 106623. <https://doi.org/10.1016/j.isci.2023.106623>.
54. Min, H., Kim, W., Hong, S., Lee, S., Jeong, J., Kim, S., and Seong, R.H. (2022). Differentiation and homeostasis of effector Treg cells are regulated by inositol polyphosphates modulating Ca(2+) influx. *Proc. Natl. Acad. Sci. USA* 119, e2121520119. <https://doi.org/10.1073/pnas.2121520119>.
55. Hong, S., Kim, K., Shim, Y.-R., Park, J., Choi, S.E., Min, H., Lee, S., Song, J.-J., Kang, S.-J., Jeong, W.-I., et al. (2024). A non-catalytic role of IPMK is required for PLCγ1 activation in T cell receptor signaling by stabilizing the PLCγ1-Sam68 complex. *Cell Commun. Signal.* 22, 526. <https://doi.org/10.1186/s12964-024-01907-0>.
56. Corry, D.B., Reiner, S.L., Linsley, P.S., and Locksley, R.M. (1994). Differential effects of blockade of CD28-B7 in the development of Th1 or Th2 effector cells in experimental leishmaniasis. *J. Immunol.* 153, 4142–4148.
57. Soong, L., Xu, J.C., Grewal, I.S., Kima, P., Sun, J., Longley, B.J., Jr., Ruddle, N.H., McMahon-Pratt, D., and Flavell, R.A. (1996). Disruption of CD40-CD40 ligand interactions results in an enhanced susceptibility to *Leishmania amazonensis* infection. *Immunity* 4, 263–273.
58. Pino, P.A., and Cardona, A.E. (2011). Isolation of brain and spinal cord mononuclear cells using percoll gradients. *J. Vis. Exp.* 48, 2348. <https://doi.org/10.3791/2348>.
59. Azevedo, C., and Saiardi, A. (2006). Extraction and analysis of soluble inositol polyphosphates from yeast. *Nat. Protoc.* 1, 2416–2422. <https://doi.org/10.1038/nprot.2006.337>.

STAR★METHODS

KEY RESOURCES TABLE

REAGENT or RESOURCE	SOURCE	IDENTIFIER
Antibodies		
phospho-STAT3	Cell Signaling Technology	Cat# 9131; RRID:AB_331586
STAT3	Cell Signaling Technology	Cat# 9139; RRID:AB_331757
phospho-Akt (Ser473)	Cell Signaling Technology	Cat# 4058; RRID:AB_331168
phospho-Akt (Thr308)	Cell Signaling Technology	Cat# 4056; RRID:AB_331163
Akt	Cell Signaling Technology	Cat# 4691; RRID:AB_915783
PI3 Kinase p110 δ	Cell Signaling Technology	Cat# 34050; RRID:AB_2799043
β -actin	Cell Signaling Technology	Cat# 4970; RRID:AB_2223172
T-bet	eBioscience	Cat# 14-5825-82; RRID:AB_763634
GATA3	Santa cruz biotechnology	Cat# sc-22206; RRID:AB_2108588
ROR γ t	Santa cruz biotechnology	Cat# sc-293150
GAPDH	Santa cruz biotechnology	Cat# sc-32233; RRID:AB_627679
Caveolin-1	Santa cruz biotechnology	Cat# sc-53564; RRID:AB_628859
HSP90	Santa cruz biotechnology	Cat# sc-13119; RRID:AB_675659
IPMK	Novus	Cat# NBP1-32250; RRID:AB_2127660
Anti-mouse CD19 – Alexa Fluor TM 700	eBioscience	Cat# 56-0193-80; RRID:AB_837082
Anti-mouse CD25 – PE	eBioscience	Cat# 12-0251-82; RRID:AB_465607
Anti-mouse CD28 (clone 37.51)	eBioscience	Cat# 16-0281-86; RRID:AB_468923
Anti-mouse CD3e (clone 145-2C11)	eBioscience	Cat# 16-0031-86; RRID:AB_468849
Anti-mouse TCR β – PerCP-Cyanine5.5	eBioscience	Cat# 45-5961-82; RRID:AB_925763
Anti-mouse CD4 – eFluor TM 450	eBioscience	Cat# 48-0042-82; RRID:AB_1272194
Anti-mouse CD4 – PE-Cyanine7	eBioscience	Cat# 25-0041-82; RRID:AB_469576
Anti-mouse CD44 – APC-eFluor TM 780	eBioscience	Cat# 47-0441-82; RRID:AB_1272244
Anti-mouse CD44 – APC	eBioscience	Cat# 17-0441-82; RRID:AB_469390
Anti-mouse CD45 – Pacific Blue	Biolegend	Cat# 103126; RRID:AB_493535
Anti-mouse CD62L - FITC	eBioscience	Cat# 11-0621-82; RRID:AB_465109
Anti-mouse CD62L – PE	eBioscience	Cat# 12-0621-82; RRID:AB_465721
Anti-mouse CD8a – APC-eFluor TM 780	eBioscience	Cat# 47-0081-82; RRID:AB_1272185
Anti-mouse Foxp3 – APC	eBioscience	Cat# 17-5773-82; RRID:AB_469457
Anti-mouse F4/80 – APC	eBioscience	Cat# 17-4801-80; RRID:AB_2784647
Anti-mouse Gr1 – FITC	eBioscience	Cat# 11-5931-81; RRID:AB_465313
Anti-mouse IFN- γ – FITC	eBioscience	Cat# 11-7311-82; RRID:AB_465412
Anti-mouse IL-17A – APC	eBioscience	Cat# 17-7179-42; RRID:AB_1582221
Anti-mouse IL-10 – FITC	eBioscience	Cat# 11-7101-82; RRID:AB_465403
Anti-mouse phospho-Akt (Thr308) – PE	BD biosciences	Cat# 558275; RRID:AB_2225329
Anti-mouse phospho-Akt (Ser473) – APC	eBioscience	Cat# 17-9715-42; RRID:AB_2573310
Anti-mouse phospho mTOR – PerCP-eFluor 710	eBioscience	Cat# 46-9718-41; RRID:AB_2573894
Anti-mouse IFN- γ mAb functional grade	eBioscience	Cat# 16-7311-85; RRID:AB_469243
Anti-mouse IL-4 mAb functional grade	eBioscience	Cat# 16-7041-85; RRID:AB_469209
Anti-mouse IL-12 mAb functional grade	eBioscience	Cat# 16-7123-85; RRID:AB_469233
Anti-Armenian Hamster IgG	Jackson ImmunoResearch	Cat# 127-005-099; RRID:AB_2338971
Chemicals, peptides, and recombinant proteins		
DPBS	Welgene	Cat# LB001-02
Percoll	GE Healthcare	Cat# 9139
RPMI 1640	Welgene	Cat# LM011-01

(Continued on next page)

Continued

REAGENT or RESOURCE	SOURCE	IDENTIFIER
RPMI 1640 nophenol	Gibco	Cat# 11835030
Brefeldin A solution (1000X)	eBioscience	Cat# 00-4506-51
PMA	Calbiochem	Cat# 16561-29-8
Ionomycin	ThermoFisher Scientific	Cat# I24222
Fixable Viability Dye eFlour 506	eBioscience	Cat# 5536
Ack lysis buffer	Gibco	Cat# 2972
Foxp3/Transcription Factor staining buffer set	eBioscience	Cat# 2280
IC Fixation buffer	eBioscience	Cat# 82-0000-49
MOG peptide 35-55	Peptron	Cat# 2217
Complete Freund's adjuvant	Sigma Aldrich	Cat# F5881-6X
Pertussis toxin	List Biological	Cat# 181
Wortmannin	MedChemExpress	Cat# HY-10197
[³ H] myo-inositol	PerkinElmer	Cat# NET114A001MC
Bt ₂ Ins(1345)P ₄ /PM	Sirius fine chemicals	Cat# 4-2-1345
Bt ₂ Ins(1456)P ₄ /PM	Sirius fine chemicals	Cat# 4-2-1456
Recombinant mouse IL-2	Peprotech	Cat# 212-12
Recombinant mouse IL-12	Peprotech	Cat# 210-12
Recombinant mouse IL-4	R&D SYSTEMS	Cat# 404-ML
Recombinant mouse IL-6	BioLegend	Cat# 575706
Recombinant mouse TGF-β	Peprotech	Cat# 100-21C
Trimethylsilyl diazomethane 2M solution in hexanes	Acros organics	Cat# 385330050
C18:0/C20:4-PtdIns(3,4,5)P ₃	Avanti Polar Lipids	Cat# 850166
C18:0/C20:4-PtdIns(4,5)P ₂	Avanti Polar Lipids	Cat# 850165
C17:0/C20:4 PI(3,4,5)P ₃	Avanti Polar Lipids	Cat# LM1906

Critical commercial assays

Mouse naive CD4 T isolation Kit	eBioscience	Cat# 8804-6824-74
CellTrace violet cell proliferation kit	Invitrogen	Cat# C34557
CBA Mouse IL-17A flex set	BD biosciences	Cat# 560283
CBA Mouse IFN-γ flex set	BD biosciences	Cat# 558296
RNeasy mini kit	QIAGEN	Cat# 74104
Mem-PER™ Plus Membrane Protein Extraction Kit	Thermo Scientific	Cat# 89842
FastStart Universal SYBR Green Master (Rox)	Roche	Cat# 04913850001
Seahorse XF Cell Mito Stress Test Kit	Agilent	Cat# 103015-100
Seahorse XF Glycolysis Stress Test Kit	Agilent	Cat# 103020-100

Deposited data

Murine bulk RNA-seq data (<i>lpmk</i> ^{fl/fl} and <i>lpmk</i> ^{ΔCD4} T cells differentiated into Th0 or Th17)	This study	GEO: GSE203137
--	------------	----------------

Experimental models: Organisms/strains

C57BL/6J	The Jackson Laboratory	Strain #:000664; RRID:IMSR_JAX:000664
B6.Cg-Tg(CD4-cre)1Cwi/BfJ	The Jackson Laboratory	Strain #:022071; RRID:IMSR_JAX:022071
B6.Cg-Tg(Lck-cre)548Jxm	The Jackson Laboratory	Strain #:003802; RRID:IMSR_JAX:003802
IPMK floxed mouse	This study	N/A

Oligonucleotides

<i>lpmk</i> fwd: TGAAGATTGGCGGAAGAGC	This study	N/A
<i>lpmk</i> rev: GCCATTGTGGAAAAACTTGG	This study	N/A
<i>Actb</i> fwd: GACAGGATGCAGAAGGGAGATTAC	This study	N/A
<i>Actb</i> rev: GCTGATCCACATCTGCTGGAA	This study	N/A
<i>Rorc</i> fwd: TGCAGGAGTAGGCCACATTAC	This study	N/A
<i>Rorc</i> rev: CCGCTGAGAGGGCTTCAC	This study	N/A

(Continued on next page)

Continued

REAGENT or RESOURCE	SOURCE	IDENTIFIER
II17a fwd: CTCCAGAACGCCCTCAGACTAC	This study	N/A
II17a rev: GGGTCTTCATTGCGGTGG	This study	N/A
II23r fwd: GCCAAGAGAACCATCCCCGA	This study	N/A
II23r rev: TCAGTGCTACAATCTCAGAGGACA	This study	N/A
Foxp3 fwd: CCCAGGAAAGACAGCAACCTT	This study	N/A
Foxp3 rev: TTCTCACAAACCAGGCCACTTG	This study	N/A
II10 fwd: GCTGGACAAACATACTGCTAAC	This study	N/A
II10 rev: ATTTCCGATAAGGCTGGCAA	This study	N/A
Recombinant DNA		
Plasmid: MIGR1-GFP	Addgene	Plasmid #27490; RRID: Addgene_27490
Plasmid: pCL-Eco	Addgene	Plasmid #12371; RRID: Addgene_12371
Plasmid: MIGR1-IPMK WT-GFP	This study	N/A
Plasmid: MIGR1-IPMK SA-GFP	This study	N/A
Plasmid: MIGR1-AtIPKβ2-GFP	This study	N/A
Software and algorithms		
Flowjo v.10.6.0	FlowJo, LLC	http://www.flowjo.com/ ; RRID: SCR_008520
BD CBA analysis software	BD biosciences	https://www.bdbiosciences.com/
Prism 9	GraphPad	http://www.graphpad.com/ ; RRID: SCR_002798
ImageJ	NIH	https://imagej.nih.gov/ij/ ; RRID: SCR_003070
Image Lab v.6.0.0	Bio-Rad laboratories	https://www.bio-rad.com/ ; RRID: SCR_014210
TopHat software tool	Johns Hopkins University Center for Computational Biology	https://ccb.jhu.edu/software/tophat/ ; RRID: SCR_013035
MeV_4_8		http://mev.tm4.org/
Other		
ACQUITY UPLC Protein BEH C4 Column	Waters	Cat# 186005590
ACQUITY ULPC Protein BEH C4	Waters	Cat# 186004623
VanGuard Pre-Column		

EXPERIMENTAL MODEL AND STUDY PARTICIPANT DETAILS

Mice

Cd4-Cre, *Lck*-Cre, *lpmk*^{fl/fl} and WT mice were on the C57BL/6 background. Mice used for experiments were 6–10 weeks old male and female mice and age-matched. Littermates were used unless stated otherwise. All mice were housed and bred in specific pathogen-free conditions and fed with a standard normal diet *ad libitum* with free access to water. All animal experimental procedures were performed in accordance with guidelines approved by the Korea Advanced Institute of Science and Technology Animal Care and Use Committee (KAIST, KA2013-32 and KA2018-52).

METHOD DETAILS

CD4⁺ T cell differentiation and proliferation *in vitro*

Naive CD4⁺ T cells were isolated from the spleen and pLNs using a mouse naive CD4⁺ enrichment kit (Invitrogen) according to the manufacturer's protocols. Followed that, CD4⁺CD25⁻CD62L^{high}CD44^{low} cells were sorted using a FACS Aria II (BD Biosciences) equipped with 405 nm, 488 nm, 633 nm lasers and an 85 μm nozzle using a purity mask. Post-sort purity was routinely >97%. Isolated T cells were plated into plates coated with 10 μg/mL anti-CD3 and 10 μg/mL anti-CD28 and cultured in RPMI 1640 (Welgene) or IMDM medium (Gibco). TCR stimulation in isolated T cells was further progressed with by incubating with 20 μg/mL anti-Armenian hamster IgG secondary antibodies for indicated times, following pre-incubation with 5 μg/mL anti-CD3, 2 μg/mL anti-CD28 antibodies. To inhibit PI3K activation, naive CD4⁺ T cells were treated with 50 nM wortmannin (MedChemExpress) concurrently with TCR stimulation. Isolated naive CD4⁺ T cells were differentiated to several Th types by different recombinant cytokines and antibodies: Th0

(5 µg/mL anti-IFN- γ , 5 µg/mL anti-IL-4 in RPMI 1640 medium), Th1 (20 ng/mL IL-12, 20 ng/mL IL-2, 5 µg/mL anti-IL-4 in RPMI 1640 medium), Th2 (50 ng/mL IL-4, 10 µg/mL anti-IL-12, 5 µg/mL anti-IFN- γ in RPMI 1640 medium) Th17 (40 ng/mL IL-6, 2 ng/mL TGF- β , 5 µg/mL anti-IFN- γ and 5 µg/mL anti-IL-4 in IMDM medium). To investigate the induction of Th17 cell differentiation by InsP₄ treatment, *lpmk*^{ACD4} CD4⁺ T cells were treated with 5 µM or 10 µM Ins(1,3,4,5)P₄ or Ins(1,4,5,6)P₄ under Th17 differentiation conditions. To assess proliferation, isolated CD4⁺ T cells were labeled with 5 mM CellTrace Violet Cell proliferation (Life technologies) per the manufacturer's protocols. Labeled T cells were activated under Th17 differentiation conditions as indicated. The T cell proliferation was assessed 72 h post-activation based on CellTrace Violet dilution by flow cytometry. The membrane and cytoplasm fractionation was performed on TCR-stimulated naive CD4⁺ T cells using the Mem-PER Plus Membrane Protein Extraction Kit (Thermo Scientific) according to the manufacturer's protocols.

Viral transduction into CD4⁺ T cells

Virus production and viral transduction into isolated naive CD4⁺ T cells were conducted following the methods described by Hong et al.⁵⁵ MIGR1-GFP retroviral DNA plasmid was transfected into HEK293T cells along with pCL-Eco viral packing vector. Viral supernatant collected from the transfected cells was used to transduce CD4⁺ T cells, which were incubated on anti-CD3/anti-CD28 antibody-coated plates for 24 h post-isolation. After 24 h of viral transduction, the media were replaced with Th17 differentiation conditioned media. Cells were then incubated for an additional 72 h on anti-CD3/anti-CD28 antibody-coated plates.

Western blot analysis

Whole-cell lysates were prepared in lysis buffer (1% NP-40, 137 mM NaCl, 20 mM Tris-HCl (pH 8.0), 2 mM EDTA, 10% glycerol, 20 mM NaVO₄, 10 mM sodium pyrophosphate, 100 mM sodium fluoride, 20 mM PMSF) containing protease inhibitor cocktail (Roche). Whole cells were incubated on ice for 20 min and collected by centrifugation at 17,000g for 15 min. The total protein concentrations were determined by the Bradford protein assay (Bio-Rad), and proteins were boiled at 95°C for 5 min with SDS sample loading buffer (60 mM Tris-HCl, 25% glycerol, 2% SDS, 14.4 mM β-mercaptoethanol, and 0.1% bromophenol blue). Cell-lysate proteins were electrophoresed on 10% SDS-PAGE gels and separated proteins were transferred onto a nitrocellulose membrane. After blocking with 5% skim milk in Tris-buffered saline (TBST, 0.1% Tween 20) for 1 h at room temperature, membranes were incubated with primary antibodies overnight at 4°C. Then, the membranes were treated with an HRP-conjugated secondary antibody for 1 h at room temperature. After each step, the membranes were rinsed three times for 10 min with TBST. The HRP signals were developed with Clarity ECL substrate (Bio-Rad) and visualized by ChemiDoc (Bio-Rad) using the Image lab program. Antibodies used in this experiment are listed in [key resources table](#).

Flow cytometry

For analysis of surface markers, cells were stained with a combination of the fluorescence-conjugated antibodies, which are listed in [key resources table](#), for 20 min at 4°C in PBS containing 0.25% BSA and 0.02% azide. Dead cells were excluded by LIVE/DEAD Fixable Dead Viability Dye (Invitrogen). For assessment of cytokine production by *in vitro* derived T cells, cells were stimulated with 50 ng/mL phorbol myristate acetate (PMA) and 500 ng/mL Ionomycin with Brefeldin A (Invitrogen; 1:1000) for 3 h then stained for CD4 and a LIVE/DEAD Fixable Dead Viability Dye (Invitrogen). Cells were then fixed and permeabilized (Invitrogen) and stained for IL-17A. For assessment of Foxp3 expression or IL-17A expression, cells were fixed and permeabilized with a Foxp3 staining kit (Invitrogen). Flow cytometry was performed on an LSRII Fortessa (BD Biosciences).

Leishmania major parasites and infectious challenge

L. major strain MRHO/SU/59/P/LV39 was cultured and used to infect mice as described.^{56,57} Seven weeks following infection, mice were sacrificed, and popLNs and spleens were harvested, minced and homogenized using CM for intracellular cytokine assay.

Intracellular cytokine staining (ICCS)

Single-cell suspensions were re-stimulated PMA (50 ng/mL; Sigma-Aldrich) and ionomycin (500 ng/mL; Sigma-Aldrich) for 5 h at 37°C in a humidified 5% CO₂ atmosphere. After stimulation, cells were stained with Fixable Viability dye (Invitrogen), APC-Cy7-conjugated anti-CD8, PE-Cy7-conjugated anti-CD4, and AF700-conjugated anti-CD44 antibodies against the corresponding cell surface proteins. Following the surface staining, samples were fixed and permeabilized using the Intracellular Fixation & Permeabilization Buffer Set from eBioscience, and intracellular IL-4 and IFN- γ were detected by immunostaining with PE-conjugated anti-IL-4 and FITC-conjugated anti-IFN- γ antibodies. Appropriate PE and FITC-conjugated, isotype-matched, irrelevant monoclonal antibodies were used as isotype controls. Flow cytometry was performed using MACSQuant (Miltenyi Biotec, Bergisch Gladbach, Germany) and data were analyzed with FlowJo software (FlowJo, LLC.).

EAE model

EAE was induced by subcutaneous immunization with 200 µg MOG_{35–55}peptide (Peptron, Daejeon, Korea) emulsified in complete Freund's adjuvant (Sigma-Aldrich), followed by intravenous injection of 200 ng pertussis toxin (Sigma-Aldrich) on days 0 and 2. To quantify disease severity, scores were assigned daily in a blinded manner on a scale of 0–5 as follows: 0, no paralysis; 0.5, clumsy gait; 1, limp tail; 2, limp tail and partial hind leg paralysis; 3, complete hind leg paralysis; 4, tetraparesis; 5, moribund. Animals were

euthanized if scores reached grade 4. To determine CNS infiltrates, cell suspensions from brain and spinal cord were prepared, as described previously.⁵⁸

Induction of experimental allergic asthma

A. oryzae protease (AP) and chicken egg ovalbumin (OVA) were purchased (Sigma-Aldrich) and reconstituted to 1 mg/mL and 0.5 mg/mL using sterile PBS. AP and OVA were mixed to prepare APO allergen at a 1:9 (v/v) ratio immediately before administration. Mice were challenged five times intranasally with 50 µL of APO allergen every 4 days (days 0, 4, 8, 12, and 16). For the intranasal challenge, mice were lightly anesthetized by isoflurane inhalation (Abbott Laboratory). After allergen challenge, AHR, bronchoalveolar lavage (BAL) cytology, BAL glyccoprotein assay, and lung histopathology were determined as previously described.²⁶

Measurement of airway hyperresponsiveness (AHR)

AHR was measured with a flexiVent system (SciTech, Montreal, Canada). Briefly, 16 h after the final intranasal challenge, mice were anesthetized with pentobarbital (Hanlim Pharma Co., Seoul, Korea) via intraperitoneal injection of 0.15 mL/10 g body weight and intubated with a 20-gauge cannula. After intubation, mice were injected with 0.1 mL/10 g body weight of pancuronium (0.1 mg/mL; Sigma-Aldrich) and ventilated with the flexiVent system. AHR was assessed by administering incremental doses of nebulizing methacholine (0, 1, 3, 9, 27, 81 mg/mL; Sigma-Aldrich) and measuring resistance every 30 s. After measuring AHR, BAL fluid (BALF) samples were obtained by washing the lungs with PBS (1 mL, 4°C) delivered via a tracheal tube.

Quantification of secreted glycoprotein

Secreted glycoprotein levels in BALF were measured by modified ELISA using jacalin, a glycoprotein-binding lectin. Briefly, a glycoprotein mucin standard derived from porcine stomach (Sigma-Aldrich) and BALF samples were diluted 2-fold serially with PBS, beginning at a 1:100 dilution. 40 µL of each sample was transferred to a flat-bottom ELISA plate (Greiner, Kremsmunster, Austria) and incubated at 4°C overnight. After washing, the plates were blocked by adding 200 µL of 0.2% I-block (Applied Biosystems) and incubating at 37°C for 2 h. Plates were washed again, then 40 µL of biotinylated jacalin (Vector Laboratories) diluted in PBS/Tween containing 0.1% BSA (1:1000 dilution) was added and the plates were incubated at room temperature for 30 min. After a final wash, 70 µL of alkaline phosphatase substrate (5 mM *p*-nitrophenyl phosphate substrate in 0.1 M alkaline buffer; Sigma-Aldrich) was added and color was allowed to fully develop. The reaction was terminated by adding 40 µL 0.5 N sodium hydroxide, and optical density was measured at 405 nm using an ELISA plate reader (Marshall Scientific).

ELISA for cytokine detection

Detection of cytokines in BALF was performed by sandwich ELISA using 96-well plates (Greiner) according to the manufacturer's instructions (BD Biosciences). Briefly, ELISA plates were pre-coated with 40 µL of 1:500-diluted capture antibody, incubated for 2 h at 37°C, and then washed and blocked with 200 µL of 0.2% I-block (Applied Biosystems) overnight at 4°C. After washing, 40 µL of the collected sample was transferred to a 96-well plate and 40 µL of 1:500-diluted detection antibody was added. After incubation for 2 h at 37°C, plates were washed again and 40 µL of streptavidin-alkaline phosphatase (BD Biosciences) diluted 1:1000 in PBS/Tween/BSA was added and plates were incubated at room temperature for 30 min. After a final wash, 70 µL of alkaline phosphatase substrate (5 M *p*-nitrophenyl phosphate substrate in 0.1 M alkaline buffer; Sigma-Aldrich) was added and plates were incubated at room temperature to allow color development. The reaction was terminated by adding 40 µL of 0.5 N sodium hydroxide, and optical density was measured at 405 nm using an ELISA plate reader (Marshall Scientific).

Lung tissue histology

For staining with PAS, mouse lungs were inflated and fixed with 4% paraformaldehyde (Sigma-Aldrich) after collection of BALF cells. Lung samples were embedded in paraffin and sectioned (6 µm thick), and then stained with PAS.

RNA isolation and quantitative RT-PCR

For qRT-PCR analysis, total RNA was extracted from T cells by using RNeasy mini kit (QIAGEN) and reverse-transcribed into cDNA with Superiorscript III reverse transcriptase (Enzyomics, Daejeon, Korea), dNTP set and oligo(dT) primer (Invitrogen) per manufacturer's protocols. Quantitative PCR (qPCR) was performed using the SYBR Green Master Mix (Roche) and the StepOnePlus Real-Time PCR System (Applied Biosystems). ΔC_t values were calculated as $2^{(\text{reference} - \text{gene})}$, where the reference was β-actin.

RNA sequencing

The alignment file was used to perform bulk RNA-sequencing of control or *lpmk*^{ACD4} T cells differentiated into Th17 cells. Briefly, the TopHat software tool was used to map reads. The alignment file was used to assemble transcripts, estimate their abundances, and use cufflinks to detect differential expression of genes or isoforms. The data were further evaluated in the context of canonical signaling using the ingenious pathway analysis program (QIAGEN) to see if *lpmk*^{ACD4} Th17 genes were specifically associated with differentiation. Heatmaps were generated using MeV (<http://www.tm4.org>). For GSEA, gene set collections from the Molecular Signatures Database 4.0 (<http://www.broadinstitute.org/gsea/msigdb/>) were used. Sequence data were deposited in the NCBI GEO (accession number GSE203137).

Cytometric bead array (CBA)

Supernatants obtained from the 3 days cultures of differentiated T cells were analyzed for Th cytokines using CBA assays. The CBA assay, performed using a kit (BD Biosciences), allows the simultaneous detection and quantification of soluble murine IFN- γ , IL-17A, and IL-17F in a single sample. The principle of the CBA assay is as follows: five bead populations of equal size but distinct fluorescence intensities (resolved in the FL3 channel of a flow cytometer) are coated with capture antibodies specific for the different cytokines and mixed to form the CBA. The cytokine capture beads are mixed with recombinant cytokine standards or test samples and then mixed with the PE-conjugated detection antibodies, which are resolved in the FL2 channel. Following acquisition of sample data by flow cytometer, the results were analyzed using the BD CBA analysis software (BD Biosciences). Standard curves, plotted using the MFI of the beads for cytokine values ranging from 0 to 5,000 pg/mL, were used for quantifying the sample cytokines.

Quantification of inositol polyphosphates

Measurement of InsPs levels using High-Performance Liquid Chromatography (HPLC) was based on methods from Azevedo et al.⁵⁹ Isolated naive CD4 $^{+}$ T cells were radiolabeled with 50 μ L/mL of [3 H] myo-inositol (PerkinElmer) for 3 days under Th17 differentiation conditions. InsPs extraction from the radiolabeled Th17 cells followed the protocols described by Kim et al.; and Min et al.^{21,54}

Quantification of PtdInsP(3,4,5)₃/PtdInsP(4,5)₂

The levels of C18:0/C20:4-PtdIns(4,5)P₂ and C18:0/C20:4-PtdIns(3,4,5)P₃ in naive CD4 $^{+}$ T cells were measured by using a liquid chromatography-tandem mass spectrometry (Nexera system, LCMS-8050, Shimadzu, Kyoto, Japan). We followed the extraction procedure and derivatization method described in Clark et al.³⁷ 1 μ L of the resulting cell extract (200 μ L) was injected onto a C4 column (UPLC BEH C4, 1.7 μ m particle size, 300 \AA pore size, 100 mm length x 1 mm inner diameter, Waters, Ireland). Solvent A consisted of deionized water containing 0.1% (v/v) formic acid. Solvent B consisted of 0.1% (v/v) formic acid in acetonitrile. We optimized the gradient conditions for the chromatography: 0–3.0 min 60% B, 3.0–5.0 min linear gradient 100% B, 5.0–7.0 min 100% B, and re-equilibration at 60% B for 2.5 min (100 μ L/min flow rate). C17:0/C20:4-PtdIns(3,4,5)P₃ standards (Avanti Polar Lipids, Alabaster, Alabama, USA) were used as an internal standard. Synthetic C18:0/C20:4-PtdIns(4,5)P₂ and C18:0/C20:4-PtdIns(3,4,5)P₃ standards (Avanti Polar Lipids) were used to determine the retention time (RT), the *m/z* values of the precursor ions, and the MS/MS fragmentation patterns.

Mitochondrial respiration and glycolysis assay

CD4 $^{+}$ T cells (2×10^5) were seeded in a 96-well plate and were stimulated with 2.5 μ g/mL of anti-CD3 antibody (clone: 145-2C11) and 0.5 μ g/mL anti-CD28 antibody (clone: 37.51). After two days of culture, cell pellets were collected for assay. Mitochondrial respiration and glycolysis were determined by measuring OCRs and ECARs in the extracellular space with a Seahorse XF96 Extracellular Flux Analyzer with the XF Cell Mito Stress Test Kit and XF Glycolysis Stress Test Kit (Seahorse Bioscience) according to the manufacturer's instructions.

QUANTIFICATION AND STATISTICAL ANALYSIS

Data analysis was performed using GraphPad Prism Software 9.0 (La Jolla, CA). Statistics were calculated using a one-sample *t* test, unpaired two-tailed Student's *t*-test, Mann-Whitney test, or one-way ANOVA. Means are given as \pm SEM, with *p* values considered significant as follows: ns, not significant; **p* < 0.05; ***p* < 0.01; ****p* < 0.001; and *****p* < 0.0001.